

Supporting Information

**Pentagon-Embedded N-Doped Coumarinacenes: Tandem Synthesis and Tunable
Photophysical Attributes for Biomolecular Probing**

Nitisha, S. Sahu and P. Venkatakrishnan

Department of Chemistry, Indian Institute of Technology Madras, Chennai - 600036,

Tamil Nadu, INDIA

pvenkat@iitm.ac.in

Table of contents

S. No.	Title	Page No.
1.	General Information	S2
2.	Experimental section	S2
3.	High Resolution Mass Spectra	S6
4.	¹ H and ¹³ C NMR Scans	S8
5.	X-ray Crystal Structure Characterization Details	S16
6.	Photophysical characterization details	S19
7.	Solvatochromism and Dipole moment calculations	S20
8.	Time-Resolved fluorescence measurements	S29
9.	Aggregation Effect	S30
10.	Fluorescence Anisotropy Studies	S31
11.	Stability and reactivity of Compound 5 under different environment conditions	S33
12.	Electrochemical Studies	S34
13.	DFT Calculated FMOs and energies	S37
14.	References	S37

1. General Information

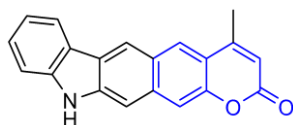
Starting materials such as diene precursor 6,7-bis(bromomethyl)-4-methylcoumarin, and dienophiles *N*-ethylindole, *N*-phenylindole, and *N*-(*p*-methoxyphenyl)indole were synthesized as reported in the literature.[1,2] Indole was procured from commercial sources and used as such. The distilled and dry solvent DMF was used as the solvent for the Diels Alder reaction. Column chromatography was performed on 100-200 silica gel mesh and thin layer chromatography (TLC) was performed to check the progress of the reaction. The newly synthesized products were characterized by ¹H and ¹³C NMR spectroscopy, recorded by a Bruker Avance 400 spectrophotometer and the chemical shifts (in ppm) referenced relative to residual protic solvent peak (CDCl₃ in particular). High resolution Q-ToF mass spectrometer was used to obtain the High-resolution mass spectra.

2. Experimental Section

General method for the Diels-Alder reaction

To a two-necked round bottom flask equipped with a magnetic stir-bar, were added 6,7-bis(bromomethyl)-4-methylcoumarin (0.050 g, 0.144 mmol), potassium iodide (0.119 g, 0.72 mmol), and dienophile (1.2 equiv.), and they were dissolved in dry DMF (1.0 mL). The contents were stirred in an oil bath at 85 °C for 24 h. The progress of the reaction was monitored by thin layer chromatography. Once the reaction was completed (as identified by TLC), the reaction mixture was poured into the cold water. The precipitates formed were filtered, washed with cold water to obtain the crude product. The crude product was then passed through a silica-gel flash column chromatography using ethyl acetate-hexane mixtures to obtain the pure product.

4-Methylchromeno[7,6-*b*]carbazol-2-(11*H*)-one, (2)

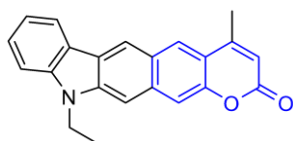


Yield: 0.006 g, 14%; yellow solid; Mp: 305-311 °C; *R*_f = 0.56 (7:3, Hexane/EtOAc); IR (KBr, cm⁻¹): 2951, 2921, 2854, 1720, 1623, 1566, 1461, 1433, 1390, 1357, 1261, 1213, 1153, 1055, 1041, 891, 754; ¹H NMR (400 MHz, CDCl₃) δ 8.65 (s, 1H), 8.31 (s, 1H), 8.19 (d, *J* = 7.6 Hz, 1H), 8.07 (s, 1H), 7.78 (s, 1H), 7.76 (s, 1H), 7.52 (t, *J* = 7.6 Hz, 1H), 7.44 (d, *J* = 7.6 Hz, 1H),

7.30 (t, $J = 7.6$ Hz, 1H), 6.31 (s, 1H), 2.60 (s, 3H); $^{13}\text{C}\{^1\text{H}\}$ NMR (100 MHz, DMSO) δ 160.6, 153.5, 149.5, 143.0, 141.8, 133.8, 128.2, 126.9, 126.0, 124.7, 122.4, 121.5, 120.3, 119.5, 117.3, 113.8, 111.2, 110.7, 104.4, 18.6; HRMS (ESI-TOF) m/z : $[\text{M} + \text{Na}]^+$ Calcd. for $\text{C}_{20}\text{H}_{13}\text{NNaO}_2$, 322.0844; found, 322.0844; ppm error: 0.000.

Synthesis of 11-ethyl-4-methylchromeno[7,6-*b*]carbazol-2(11*H*)-one, (3)[1]

Into a round bottom flask, potassium hydroxide (0.022 g, 0.40 mmol) was suspended in DMF (2.0 mL), and to the stirred solution, was added compound **2** (0.040 g, 0.13 mmol) followed by the addition of ethyl bromide (0.029 g, 0.27 mmol). The reaction mixture was stirred at room temperature for 3 h. The progress of the reaction was monitored by TLC. On completion, the ice water was added into the reaction mixture and the organic content was extracted into chloroform. The anhydrous sodium sulphate was added into the extracted organic layer, filtered and the organic layer was concentrated using rotary evaporator. The crude product was collected and passed through the silica-gel column chromatography using ethyl acetate-hexane mixtures to obtain the purified yellow product.



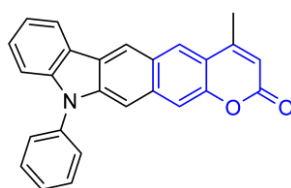
Yield: 0.022 g, 50%; yellow solid; Mp: 248-250 °C; $R_f = 0.34$ (17:3; Hexane/EtOAc); IR (KBr, cm^{-1}): 2975, 2953, 2925, 2852, 1720, 1625, 1605, 1486, 1472, 1329, 1229, 1181, 1056, 927, 748; ^1H NMR (400 MHz, CDCl_3) δ 8.62 (s, 1H), 8.27 (s, 1H), 8.19 (d, $J = 8.0$ Hz, 1H), 7.79 (s, 1H), 7.63 (s, 1H), 7.56 (t, $J = 8.0$ Hz, 1H), 7.39 (d, $J = 8.0$ Hz, 1H), 7.28 (t, $J = 7.6$ Hz, 1H), 6.28 (s, 1H), 4.39 (q, $J = 7.2$ Hz, 2H), 2.58 (s, 3H), 1.50 (t, $J = 7.2$ Hz, 3H); $^{13}\text{C}\{^1\text{H}\}$ NMR (100 MHz, CDCl_3) δ 161.5, 152.4, 149.9, 142.9, 141.8, 133.9, 127.9, 126.0, 125.8, 124.8, 122.7, 121.2, 120.0, 119.5, 117.6, 114.3, 111.4, 108.5, 101.9, 37.9, 18.8, 13.4; HRMS (ESI-TOF) m/z : $[\text{M} + \text{H}]^+$ Calcd. for $\text{C}_{22}\text{H}_{18}\text{NO}_2$, 328.1338; found, 328.1321; ppm error: -5.181.

General procedure for the synthesis of compounds **4** and **5**[2]

To a two-neck round bottom flask equipped with a stir-bar and nitrogen balloon, were added compound **2** (0.020 g, 0.07 mmol), potassium carbonate (0.025 g, 0.18 mmol), copper iodide (0.008 g, 0.04 mmol), and 1,10-phenanthroline (0.002 g, 0.007 mmol). The contents were suspended into DMF (0.4 mL). The suspension was purged with a nitrogen gas for 5 minutes and then aryl iodide (0.134 mmol) was added. The mixture was then stirred in an oil bath

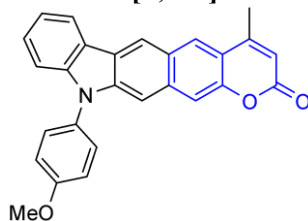
overnight at 90 °C. After monitoring the reaction progress and noting the reaction completion by TLC, the reaction was quenched by adding ice-water to it. The organic portion was extracted into ethyl acetate. The organic layer was now washed with brine solution, dried over anhydrous sodium sulphate and filtered. Further, the organic layer was concentrated at a rotary evaporator to collect the crude product. The crude product mixture was passed through the silica-gel column chromatography using ethyl acetate-hexane mixtures to afford the pure product in good yield.

4-Methyl-11-phenylchromeno[7,6-*b*]carbazol-2(11*H*)-one, (4)



Yield: 0.014 g, 55%; yellow solid; Mp: 249–251 °C; R_f = 0.28 (17:3, Hexane/EtOAc); IR (KBr, cm^{-1}): 2925, 2854, 1730, 1717, 1687, 1626, 1600, 1500, 1467, 1381, 1346, 1226, 1059, 934, 749; ^1H NMR (400 MHz, CDCl_3) δ 8.69 (s, 1H), 8.32 (s, 1H), 8.25 (d, J = 8.0 Hz, 1H), 7.61–7.71 (m, 6H), 7.55 (t, J = 7.2 Hz, 1H), 7.48 (t, J = 7.2 Hz, 1H), 7.37 (d, J = 8.0 Hz, 1H), 7.34 (t, J = 7.2 Hz, 1H), 6.30 (s, 1H), 2.60 (s, 3H); ^{13}C $\{^1\text{H}\}$ NMR (100 MHz, CDCl_3) δ 161.3, 152.3, 149.8, 143.7, 142.6, 137.4, 134.0, 130.3, 128.1, 128.0, 127.3, 126.0, 125.7, 125.4, 122.9, 121.1, 120.6, 119.8, 118.0, 114.5, 111.5, 109.8, 103.4, 18.8; HRMS (ESI-TOF) m/z : $[\text{M} + \text{H}]^+$ Calcd. for $\text{C}_{26}\text{H}_{18}\text{NO}_2$, 376.1338; found, 376.1322; ppm error: -4.254.

11-(4-Methoxyphenyl)-4-methylchromeno[7,6-*b*]carbazol-2(11*H*)-one, (5)



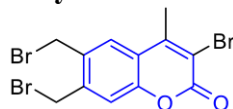
Yield: 0.015 g, 53%; yellow solid; Mp: 251–253 °C; R_f = 0.43 (4:1, Hexane/EtOAc); IR (KBr, cm^{-1}): 2955, 2925, 2851, 1731, 1627, 1514, 1468, 1449, 1249, 1227, 1184, 1032, 749; ^1H NMR (400 MHz, CDCl_3) δ 8.66 (s, 1H), 8.29 (s, 1H), 8.23 (d, J = 7.6 Hz, 1H), 7.66 (s, 1H), 7.55 (s, 1H), 7.45–7.52 (m, 3H), 7.32 (t, J = 7.6 Hz, 1H), 7.28 (d, J = 7.6 Hz, 1H), 7.17 (d, J = 8.8 Hz, 2H), 6.28 (s, 1H), 3.95 (s, 3H), 2.58 (s, 3H); ^{13}C $\{^1\text{H}\}$ NMR (100 MHz, CDCl_3) δ 161.4, 159.4, 152.3, 149.8, 144.3, 143.2, 134.0, 129.9, 128.8, 128.0, 126.0, 125.8, 125.3, 122.7, 121.1, 120.3, 119.9, 117.9, 115.5, 114.5, 111.5, 109.7, 103.4, 55.8, 18.9; HRMS (ESI-TOF) m/z : $[\text{M} + \text{H}]^+$

Calcd. for C₂₇H₂₀NO₃, 406.1443; found, 406.1424; ppm error: -4.678.

Procedure for the synthesis of compound 6[3]

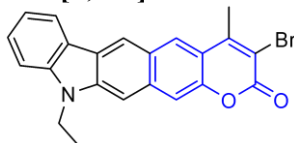
To a single-neck 50 mL round-bottom flask, compound 1 (0.344 g, 1 mmol), sodium bromide (0.247 g, 2.4 mmol) and oxone (0.304 g, 2 mmol) were added and mixed using the glass rod. The mixture turned orange color and the same was stirred and heated in an oil bath at 50 °C. Using TLC, the progress of the reaction was monitored. Adding another portion of the sodium bromide and oxone could not forward the reaction into product formation. After 1 hour, the reaction was stopped. The reaction was quenched by the addition of water. The organic components were extracted into chloroform, washed with brine solution and then dried over anhydrous sodium sulphate. The organic layer was concentrated at the rotary evaporator and the crude product was obtained. The product was further purified by silica-gel column chromatography using ethyl acetate-hexane mixtures to afford the pure product.

3-Bromo-6,7-bis(bromomethyl)-4-methyl-2H-chromen-2-one, (6)



Yield: 0.216 g, 59%; white solid; Mp: 205–208 °C; R_f = 0.29 (9:1, Hexane/EtOAc); IR (KBr, cm⁻¹): 3069, 3037, 2921, 2855, 1725, 1601, 1378, 1214, 1059, 958, 887, 747, 617; ¹H NMR (400 MHz, CDCl₃) δ 7.65 (s, 1H), 7.36 (s, 1H), 4.71 (s, 2H), 4.67 (s, 2H), 2.64 (s, 3H); ¹³C {¹H} NMR (100 MHz, CDCl₃) δ 156.4, 151.8, 150.1, 140.9, 133.4, 127.7, 120.3, 119.4, 114.5, 29.0, 28.5, 19.6; HRMS (ESI-TOF) m/z : [M + H]⁺ Calcd. for C₁₂H₁₀Br₃O₂, 422.8231; found, 422.8209; ppm error: -5.203.

3-Bromo-11-ethyl-4-methylchromeno[7,6-b]carbazol-2(11H)-one, (7)



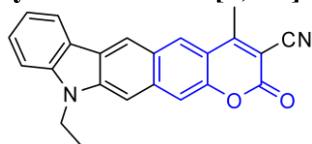
Yield: 0.021 g, 20%; orange solid; Mp: 258-260 °C; R_f = 0.6 (7:3, Hexane/EtOAc); IR (KBr, cm⁻¹): 2926, 2858, 1729, 1611, 1462, 1374, 1217, 1070, 962, 752; ¹H NMR (400 MHz, CDCl₃) δ 8.65 (s, 1H), 8.34 (s, 1H), 8.20 (d, J = 8.0 Hz, 1H), 7.81 (s, 1H), 7.64 (s, 1H), 7.58 (t, J = 8.0 Hz, 1H), 7.40 (d, J = 8.0 Hz, 1H), 7.30 (t, J = 8.0 Hz 1H), 4.41 (q, J = 7.2 Hz, 2H), 2.77 (s, 3H), 1.50 (t, J = 7.2 Hz, 3H); ¹³C {¹H} NMR (125 MHz, CDCl₃) δ 157.4, 151.0, 148.3, 142.9, 142.0, 133.8, 128.1, 126.3, 125.0, 122.6, 121.3, 120.1, 119.7, 117.3, 111.8, 111.4, 108.6, 101.9,

37.9, 19.7, 13.4; HRMS (ESI-TOF) m/z : $[M + H]^+$ Calcd. for $C_{22}H_{16}BrNO_2K$, 444.0001; found, 443.9998; ppm error: -0.676.

Procedure for the synthesis of compound 8[4]

To a 5 mL round bottom flask, compound 7 (0.010 g, 0.028 mmol) was dissolved in 0.2 mL of *N*-methyl-2-pyrrolidone. Copper cyanide (0.005 g, 0.06 mmol) was introduced later. The reaction mixture was stirred at 180 °C in an oil bath. The reaction progress was estimated by TLC monitoring and the reaction was stopped after 1 hour. The reaction mixture was passed through the celite-pad and the residues were washed with chloroform. The collected organic layer was concentrated under vacuum at rotary evaporator. The compound was further purified by silica-gel column chromatography using ethyl acetate-hexane mixtures.

11-Ethyl-4-methyl-2-oxo-2,11-dihydrochromeno[7,6-*b*]carbazole-3-carbonitrile, (8)



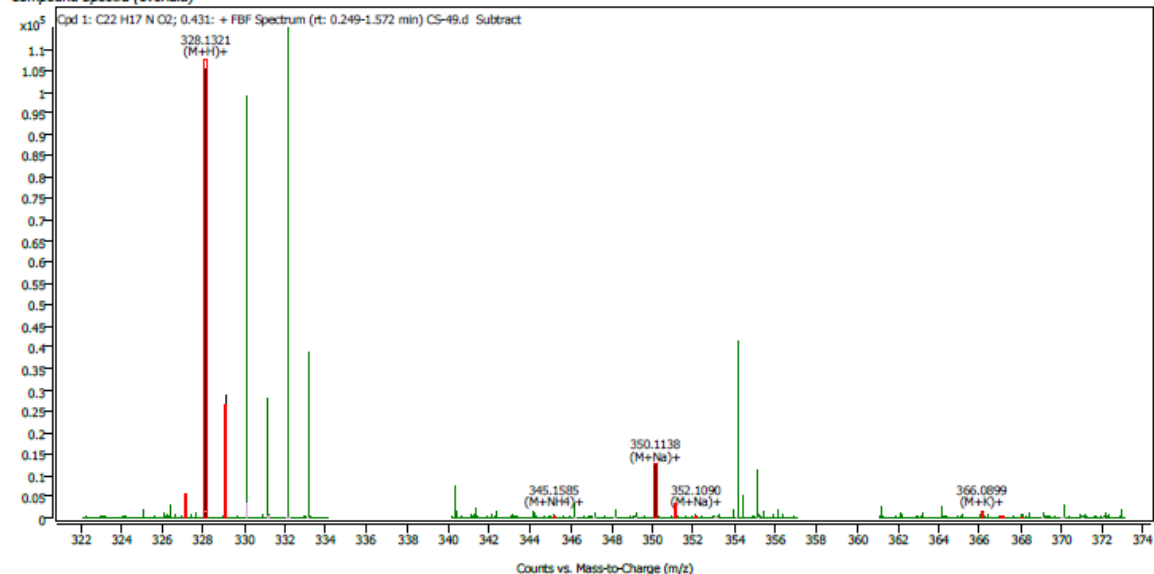
Yield: 0.002 g, 20%; red solid; Mp: 162-165 °C; R_f = 0.29 (4:1, Hexane/EtOAc); IR (KBr, cm^{-1}): 2952, 2925, 2872, 2855, 2366, 2343, 2330, 2227, 1731, 1717, 1619, 1557, 1542, 1456, 1376, 1338, 1233, 1189, 898, 746; 1H NMR (400 MHz, $CDCl_3$) δ 8.70 (s, 1H), 8.48 (s, 1H), 8.22 (d, J = 7.2 Hz, 1H), 7.83 (s, 1H), 7.68 (s, 1H), 7.61 (t, J = 7.2 Hz, 1H), 7.44 (d, J = 7.2 Hz, 1H), 7.33 (t, J = 7.2 Hz, 1H), 4.43 (q, J = 7.2 Hz, 2H), 2.93 (s, 3H), 1.50 (t, J = 7.2 Hz, 3H); ^{13}C { 1H } NMR (125 MHz, $CDCl_3$) δ 157.5, 148.6, 131.8, 131.2, 130.4, 128.8, 128.6, 126.5, 122.4, 121.5, 121.1, 120.2, 114.3, 111.9, 108.8, 102.2, 38.1, 18.3, 13.4; Poor signal to noise ratio in ^{13}C NMR spectrum is due to its poor solubility. HRMS (ESI-TOF) m/z : $[M + H]^+$ Calcd. for $C_{23}H_{17}N_2O_2$, 353.1290; found, 353.1279; ppm error: -3.115.

3. High Resolution Mass Spectra

Compound Details

Cpd. 1: C₂₂H₁₇N O₂

Compound Spectra (overlaid)



Compound ID Table

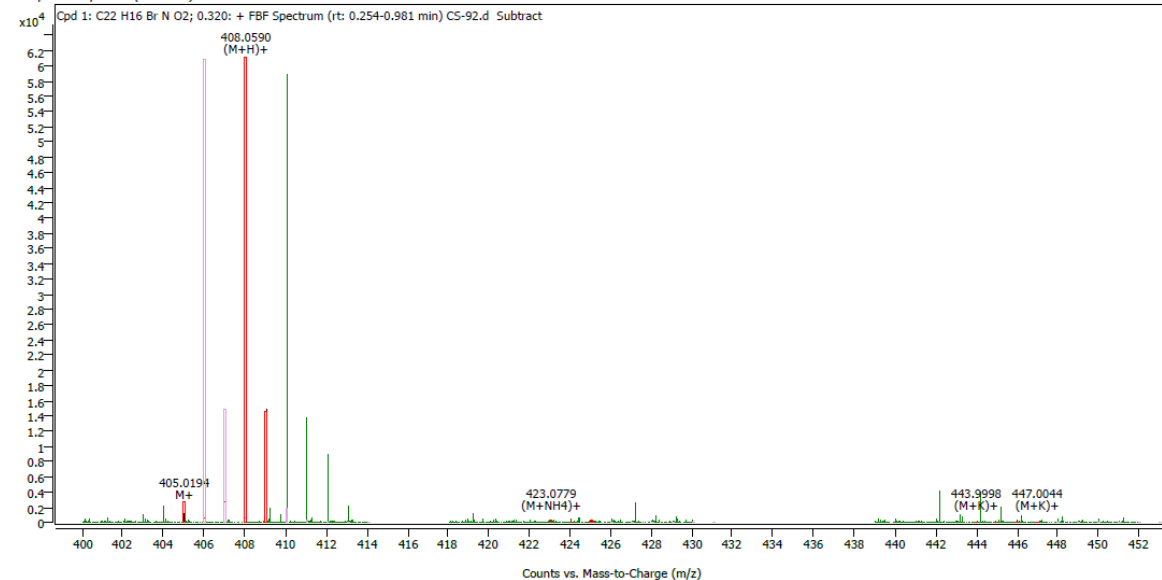
Cpd	Formula	Mass (Tgt)	Calc. Mass	Mass	Species	Diff(Tgt.ppm)	mDa
1	C ₂₂ H ₁₇ N O ₂	327.1259	327.1249	327.1249	M+ (M+H) ⁺	-3.05	-1.00
				328.1321	(M+NH ₄) ⁺		
				345.1585	(M+Na) ⁺		
				350.1138	(M+K) ⁺		

Fig. S1 HR-MS spectrum of compound 3.

Compound Details

Cpd. 1: C₂₂H₁₆Br N O₂

Compound Spectra (overlaid)



Compound ID Table

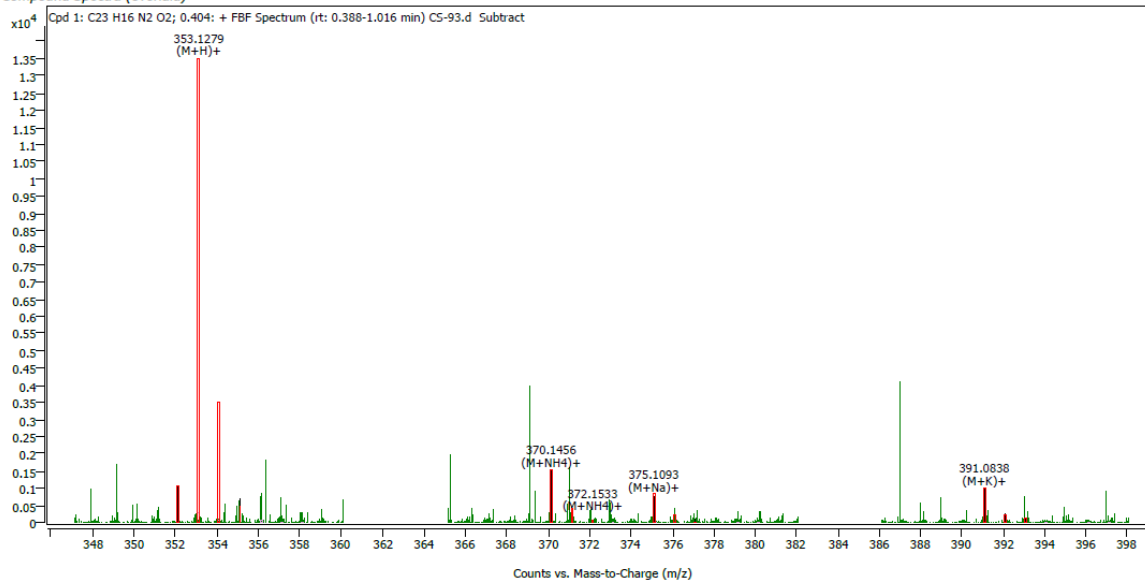
Cpd	Formula	Mass (Tgt)	Calc. Mass	Mass	Species	Diff(Tgt.ppm)	mDa
1	C ₂₂ H ₁₆ Br N O ₂	405.0364	405.0528	405.0194	M+ (M+H) ⁺	40.28	16.31
				408.0590	(M+NH ₄) ⁺		
				423.0779	(M+K) ⁺		
				443.9998	(M+K) ⁺		

Fig. S2 HR-MS spectrum of compound 7.

Compound Details

Cpd. 1: C₂₃ H₁₆ N₂ O₂

Compound Spectra (overlaid)



Compound ID Table

Cpd	Formula	Mass (Tgt)	Calc. Mass	Mass	Species	Diff(Tgt.ppm)	mDa
1	C ₂₃ H ₁₆ N ₂ O ₂	352.1212	352.1199	352.1203	M+ (M+H) ⁺	-3.62	-1.27
				353.1279	(M+NH ₄) ⁺		
				370.1456	(M+Na) ⁺		
				375.1093	(M+K) ⁺		
				391.0838			

Fig. S3 HR-MS spectrum of compound **8**.

4. ^1H and ^{13}C NMR Scans

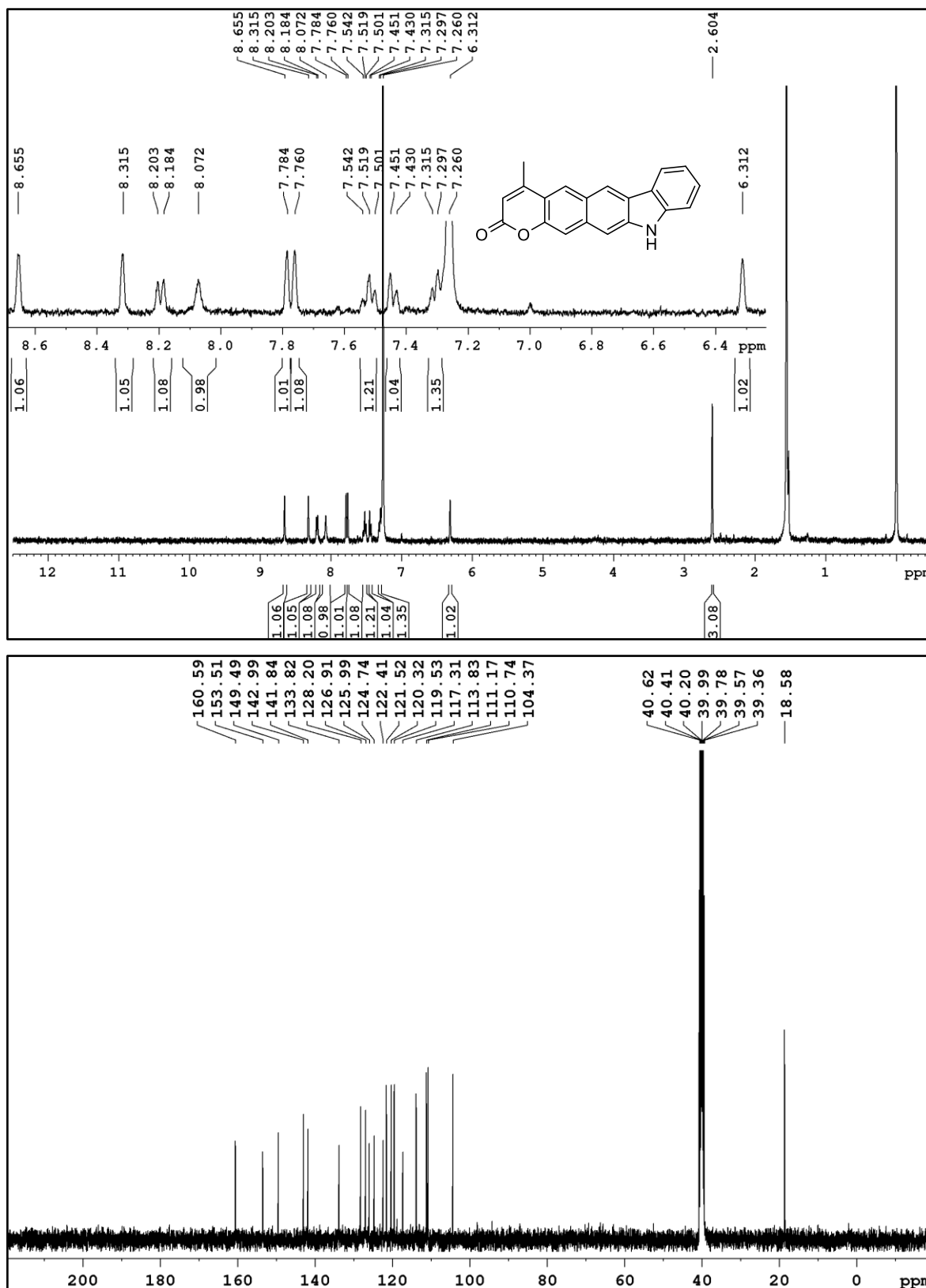


Fig. S4 ^1H and ^{13}C NMR spectra of **2** in CDCl_3 and DMSO , respectively.

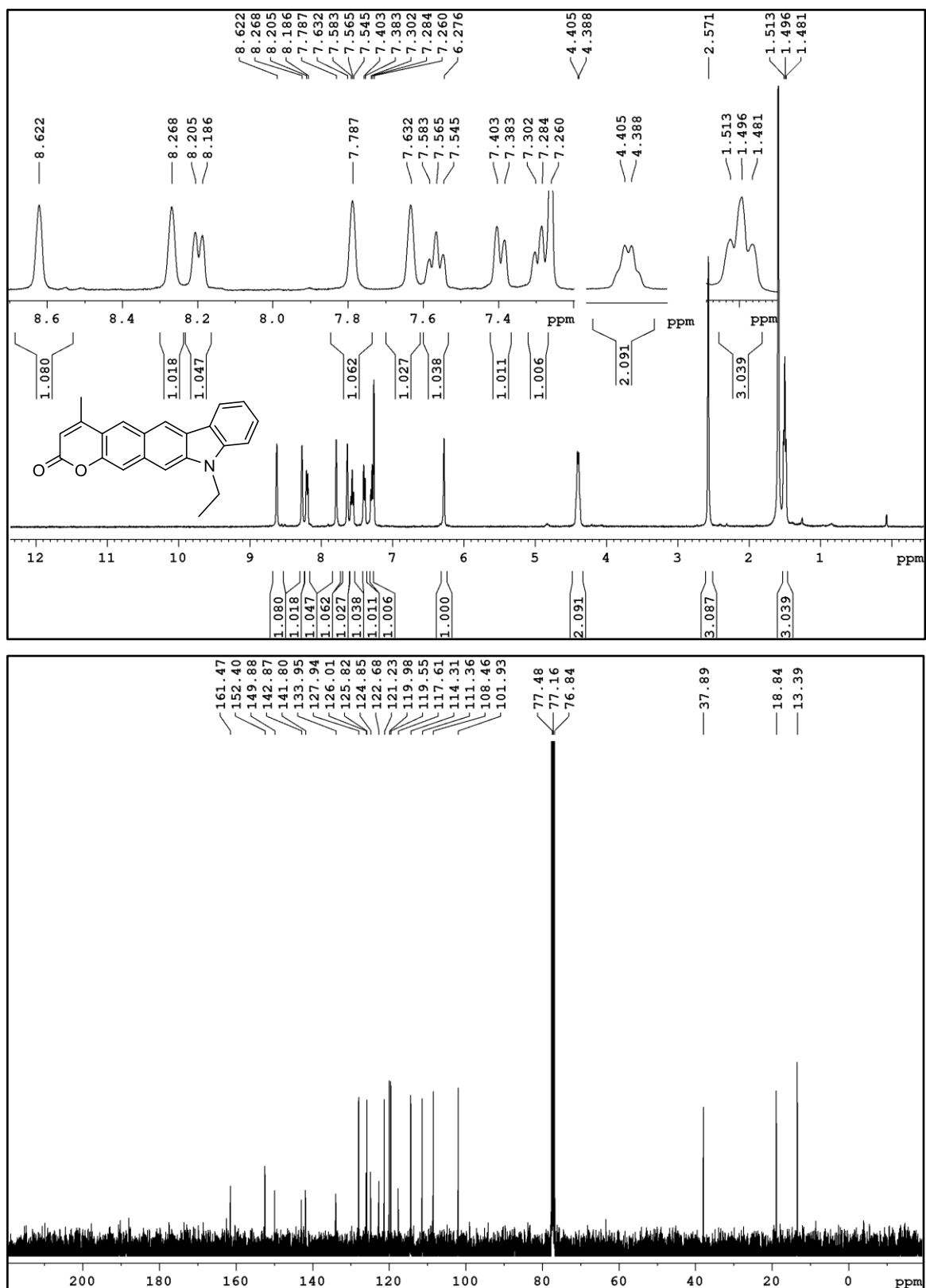


Fig. S5 ¹H and ¹³C NMR spectra of **3** in CDCl₃.

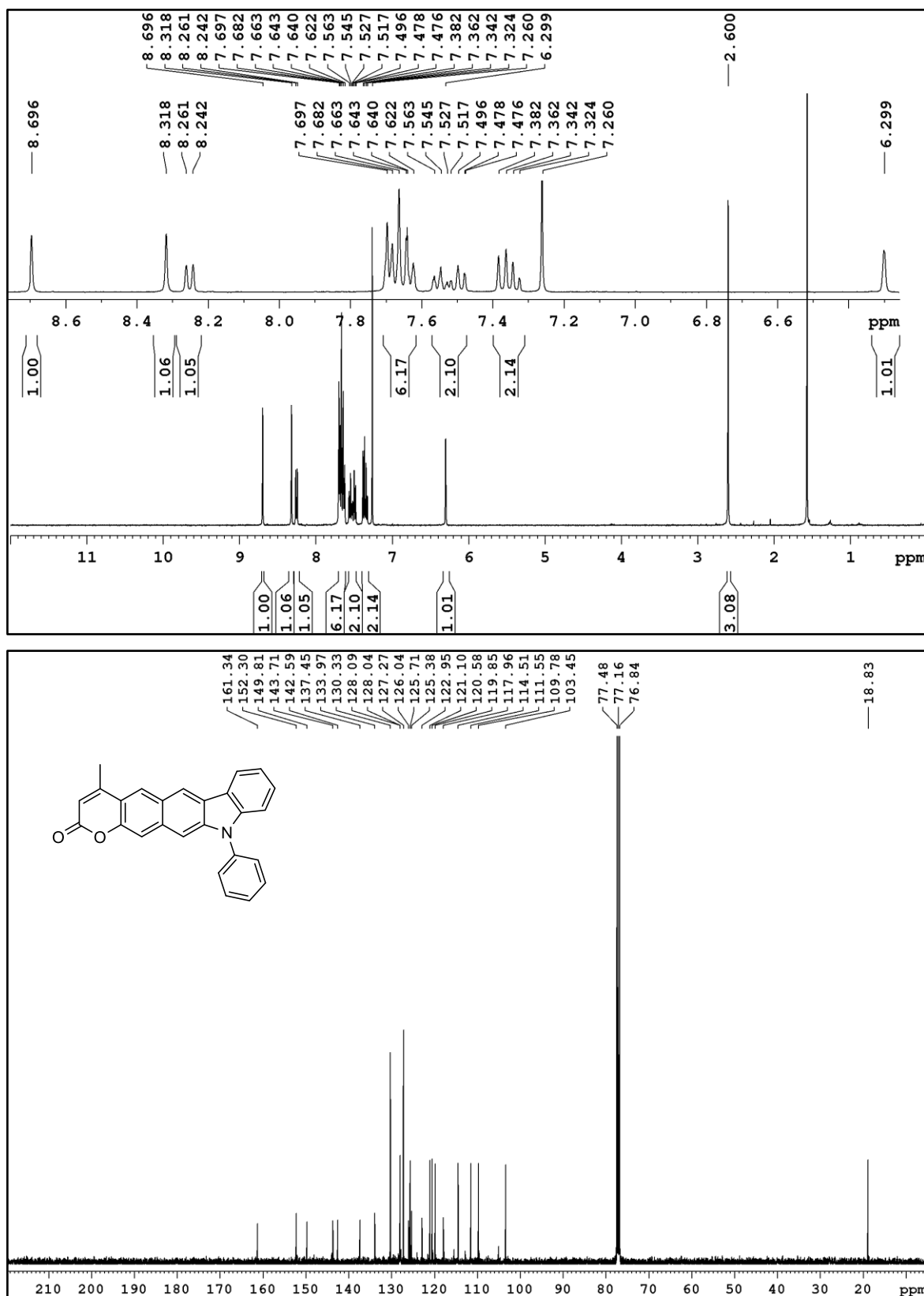


Fig. S6 ¹H and ¹³C NMR spectra of 4 in CDCl₃.

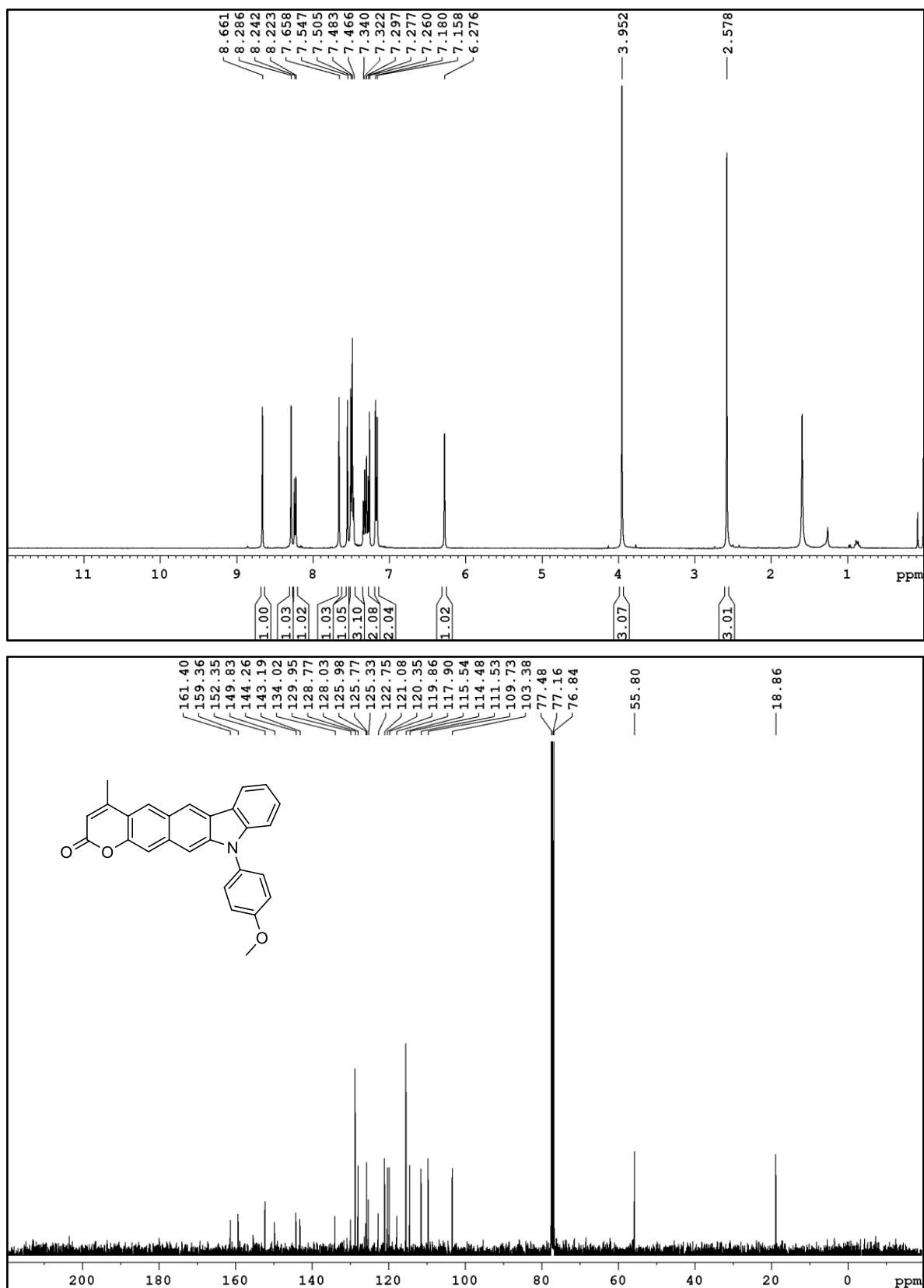


Fig. S7 ¹H and ¹³C NMR spectra of **5** in CDCl₃.

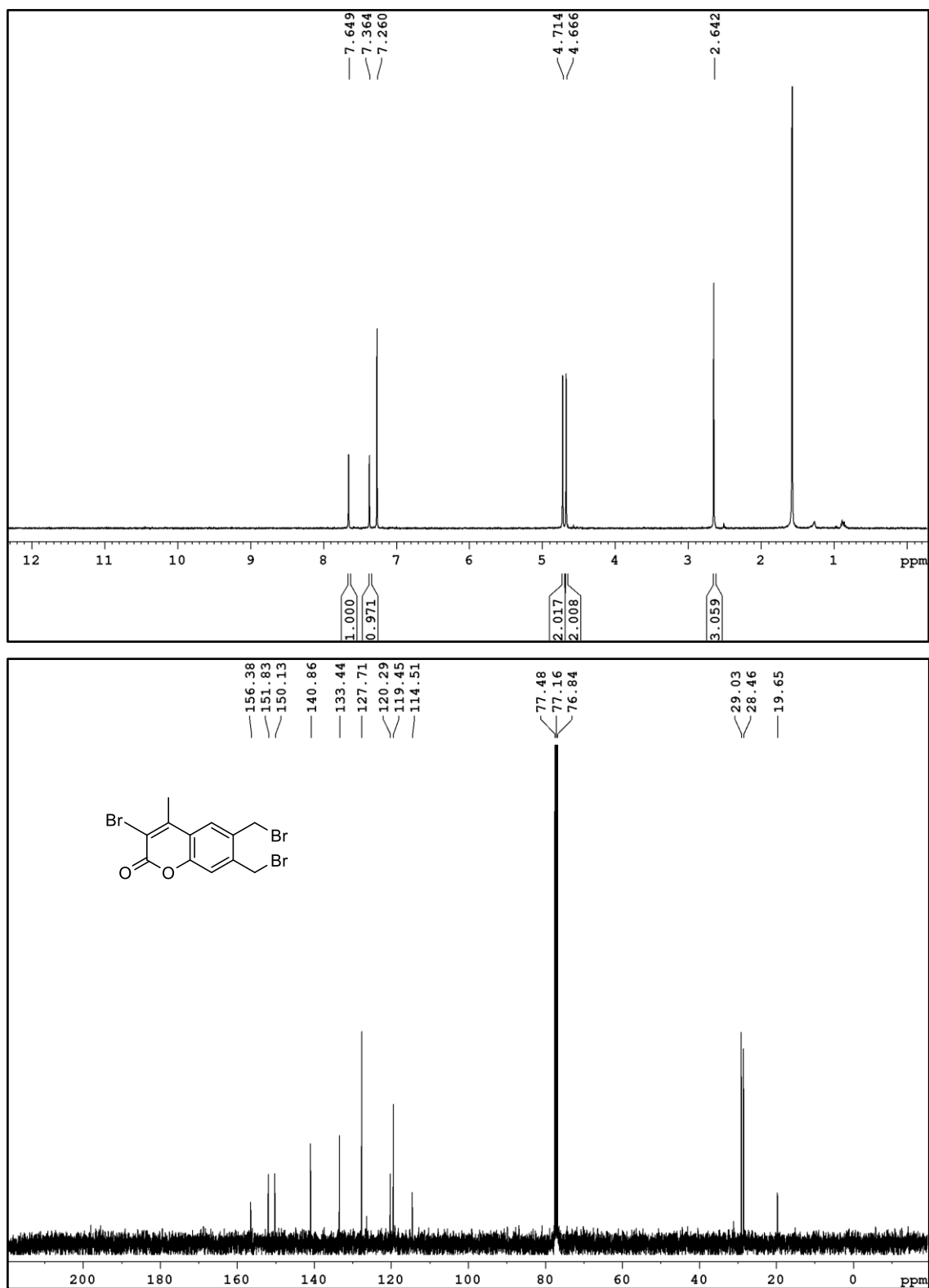


Fig. S8 ¹H and ¹³C NMR spectra of **6** in CDCl₃.

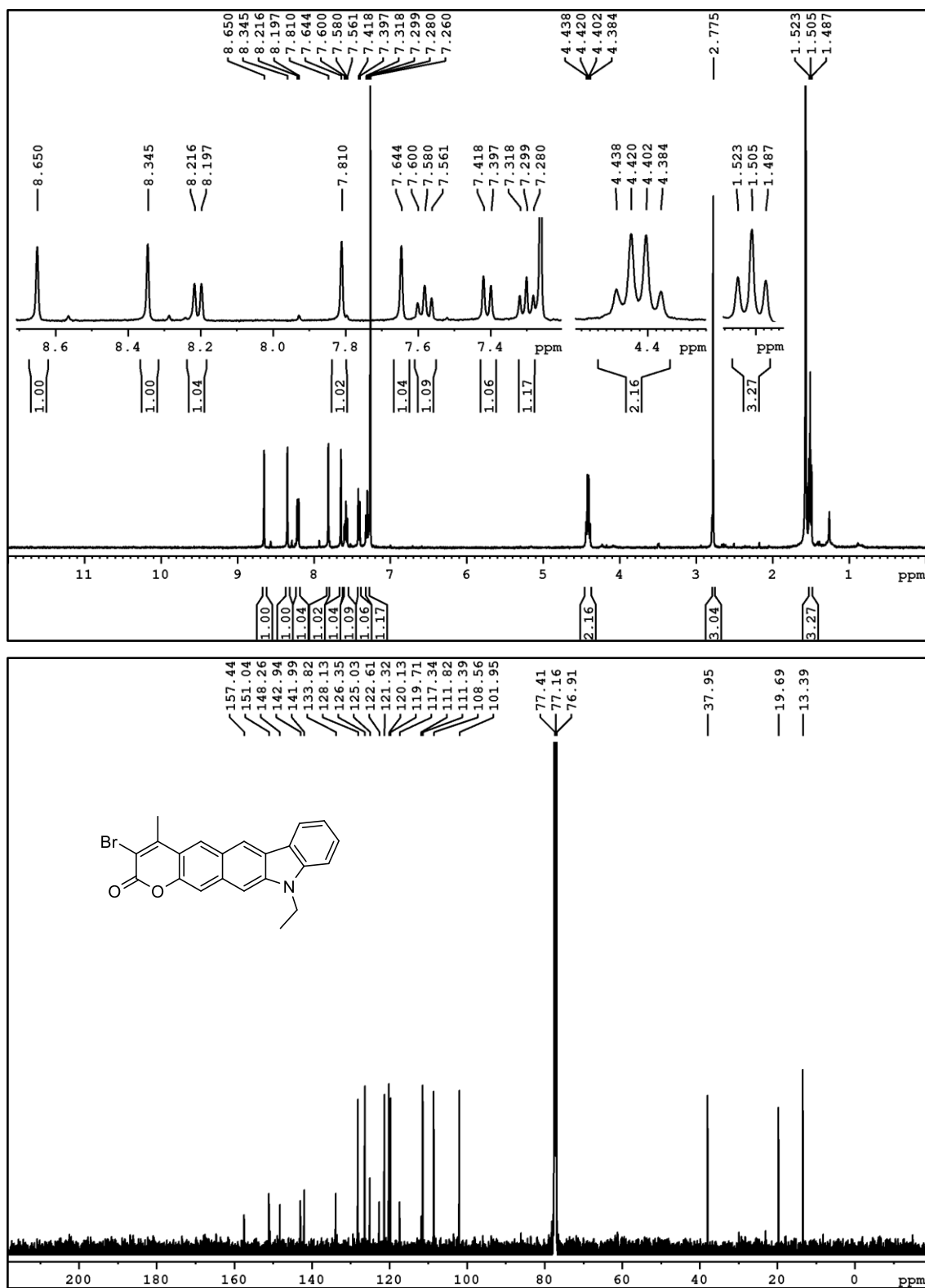


Fig. S9 ¹H and ¹³C NMR spectra of 7 in CDCl₃.

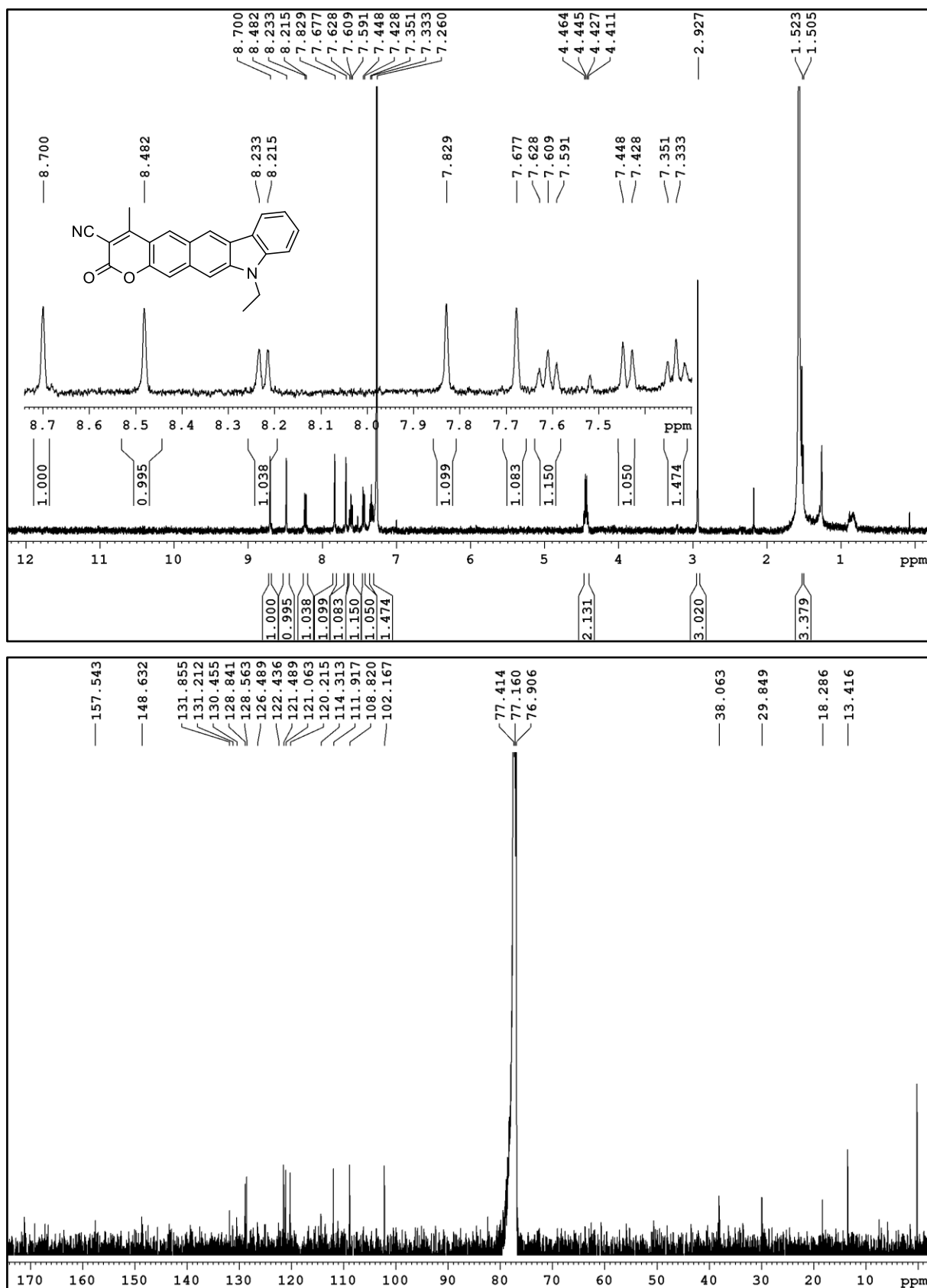


Fig. S10 ¹H and ¹³C NMR spectra of **8** in CDCl₃.

5. X-ray Crystal Structure Characterization Details

The single crystals of **3** and **4** suitable for X-ray determination were grown by slow evaporation of their solution in toluene. The transparent crystal was chosen and mounted along its longest dimension. The X-ray intensity data for **2** was collected on Bruker AXS (Kappa Apex 2) CCD diffractometer equipped with a graphite monochromated MoK α ($\lambda = 0.7107 \text{ \AA}$) radiation source at 297 K. The multi-scan absorption correction was applied to the dataset using the program SADABS.[5] The structures were solved by direct method and was refined on F² by a full-matrix least squares technique using SHELXL-2014.[6]

Table S1. Crystal data and structure refinement for compound **3**.

Identification code	shelx (CCDC 2175751)	
Empirical formula	C ₂₂ H ₁₇ NO ₂	
Formula weight	327.36 g/mol	
Temperature	297(2) K	
Wavelength	0.71073 \AA	
Crystal system	Monoclinic	
Space group	P 21/n	
Unit cell dimensions	a = 16.9636(8) \AA	$\alpha = 90^\circ$
	b = 5.4254(2) \AA	$\beta = 108.262(2)^\circ$
	c = 18.4927(8) \AA	$\gamma = 90^\circ$
Volume	1616.24(12) \AA^3	
Z	4	
Density (calculated)	1.345 g/cm ³	
Absorption coefficient	0.086 mm ⁻¹	
F(000)	688	
Crystal size	0.309 x 0.135 x 0.024 mm	
Theta range for data collection	3.603 to 26.999 $^\circ$.	
Index ranges	-21 \leq h \leq 21, -6 \leq k \leq 6, -23 \leq l \leq 23	
Reflections collected	36607	
Independent reflections	3517 [R(int) = 0.0640]	
Completeness to theta = 25.242 $^\circ$	99.8 %	
Absorption correction	Semi-empirical from equivalents	
Max. and min. transmission	0.745 and 0.690	
Refinement method	Full-matrix least-squares on F ²	
Data / restraints / parameters	3517 / 0 / 226	
Goodness-of-fit on F ²	1.072	
Final R indices [I $>$ 2 σ (I)]	R ₁ = 0.0690, wR ₂ = 0.1820	
R indices (all data)	R ₁ = 0.0920, wR ₂ = 0.1990	
Extinction coefficient	n/a	
Largest diff. peak and hole	0.331 and -0.361 e.	

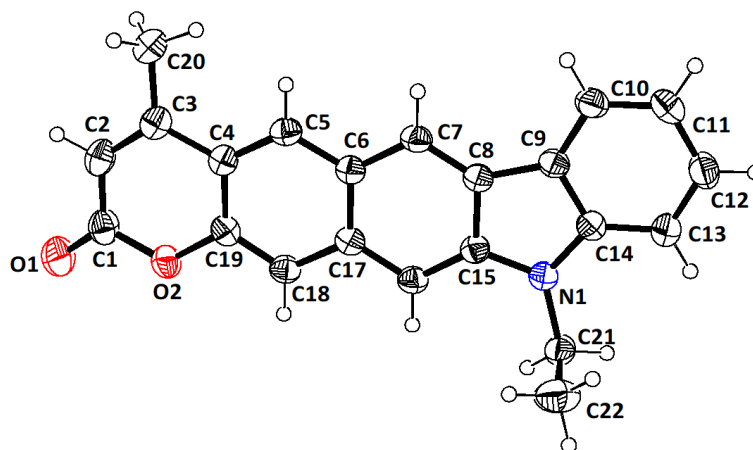


Fig. S11 The ORTEP diagram of **3** drawn at 40% probability level.

Table S2. Crystal data and structure refinement for compound **4**.

Identification code	141 (CCDC 2292825)	
Empirical formula	$C_{26}H_{17}NO_2$	
Formula weight	375.40 g/mol	
Temperature	296(2) K	
Wavelength	0.71073 Å	
Crystal system	Triclinic	
Space group	P -1	
Unit cell dimensions	$a = 7.6312(4)$ Å	$\alpha = 72.286(3)^\circ$
	$b = 9.6106(5)$ Å	$\beta = 81.389(3)^\circ$
	$c = 12.8959(8)$ Å	$\gamma = 88.455(3)^\circ$
Volume	$890.62(9)$ Å ³	
Z	2	
Density (calculated)	1.400 g/cm ³	
Absorption coefficient	0.089 mm ⁻¹	
F(000)	392	
Crystal size	0.100 x 0.150 x 0.250 mm	
Theta range for data collection	2.23 to 25.00°	
Index ranges	-9 ≤ h ≤ 8, -11 ≤ k ≤ 11, -15 ≤ l ≤ 15	
Reflections collected	12192	
Independent reflections	3140 [R(int) = 0.0244]	
Coverage of independent reflections	99.9%	
Absorption correction	multi-scan	
Max. and min. transmission	0.9910 and 0.9780	
Refinement method	Full-matrix least-squares on F^2	
Refinement program	SHELXL-2014/7 (Shedrick, 2014)	
Function minimized	$\Sigma w(F_o^2 - F_c^2)^2$	
Data / restraints / parameters	3140 / 0 / 264	
Goodness-of-fit on F^2	1.026	

Final R indices	2442 data; $I > 2\sigma(I)$	$R_1 = 0.0379$, $wR_2 = 0.0905$
	all data	$R_1 = 0.0533$, $wR_2 = 0.1020$
		$w = 1/[\sigma^2(F_o^2) + (0.0474P)^2 + 0.1963P]$
Weighting scheme		where $P = (F_o^2 + 2F_c^2)/3$
Extinction coefficient		0.0074(17)
Largest diff. peak and hole		0.215 and -0.167 $e\text{\AA}^{-3}$
R.M.S. deviation from mean		0.035 $e\text{\AA}^{-3}$

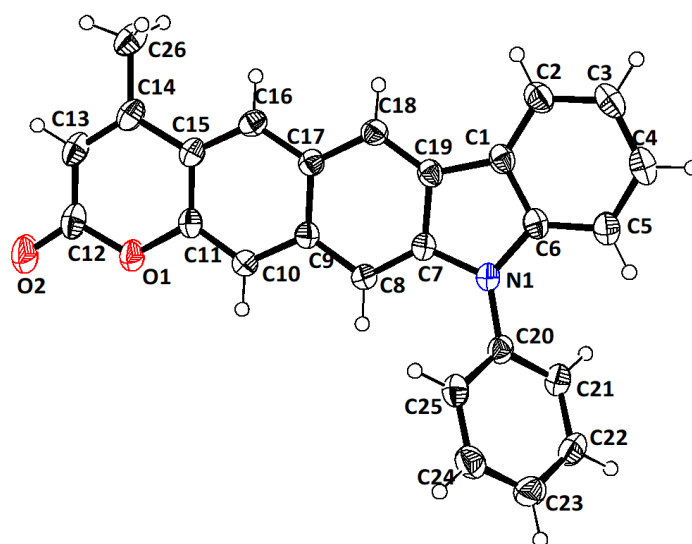


Fig. S12 The ORTEP diagram of **4** drawn at 40% probability level.

Table S3. Crystal data and structure refinement for compound **9**.

Identification code	shelx (CCDC 2292833)	
Empirical formula	$C_{20}H_{17}NO_2$	
Formula weight	303.35 g/mol	
Temperature	296(2) K	
Wavelength	0.71073 \AA	
Crystal system	Triclinic	
Space group	P -1	
Unit cell dimensions	$a = 7.7256(4) \text{\AA}$	$\alpha = 66.390(2)^\circ$
	$b = 9.6168(6) \text{\AA}$	$\beta = 77.927(2)^\circ$
	$c = 11.7022(7) \text{\AA}$	$\gamma = 83.497(2)^\circ$
Volume	$778.60(8) \text{\AA}^3$	
Z	2	
Density (calculated)	1.294 g/cm^3	
Absorption coefficient	0.084 mm^{-1}	
F(000)	320	
Crystal size	0.150 x 0.150 x 0.100 mm	
Theta range for data collection	3.022 to 28.326 $^\circ$	
Index ranges	$-10 \leq h \leq 10$, $-12 \leq k \leq 12$, $-15 \leq l \leq 15$	
Reflections collected	26625	

Independent reflections	3849 [R(int) = 0.0494]
Coverage of independent reflections	98.9%
Absorption correction	semi-empirical from equivalents
Max. and min. transmission	0.7457 and 0.6531
Refinement method	Full-matrix least-squares on F^2
Refinement program	SHELXL-2014/7 (Shedrick, 2014)
Function minimized	$\Sigma w(F_o^2 - F_c^2)^2$
Data / restraints / parameters	3849 / 0 / 216
Goodness-of-fit on F^2	1.035
Final R indices	2442 data; $I > 2\sigma(I)$ $R_1 = 0.0665$, $wR_2 = 0.1763$ all data $R_1 = 0.0957$, $wR_2 = 0.2102$
Extinction coefficient	n/a
Largest diff. peak and hole	0.467 and -0.418 $e\text{\AA}^{-3}$

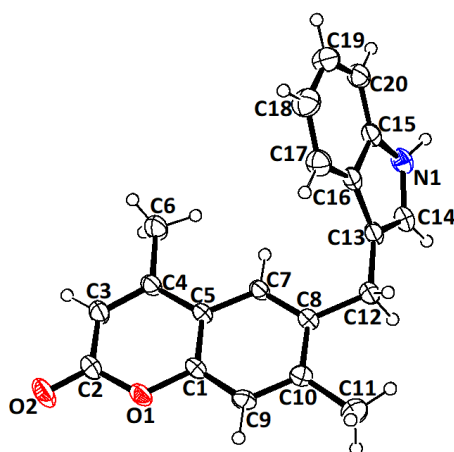


Fig. S13 The ORTEP diagram of **9** drawn at 40% probability level.

6. Photophysical Characterization Details

Steady State Absorption Measurements.

The absorption spectra of compounds were recorded on a Agilent Technologies Cary 8454 spectrophotometer for (ca. 1.0×10^{-6} M) solutions at room temperature using cuvette of path-length 1.0 cm. The molar extinction coefficient of these compounds was obtained by three independent absorbance measurements of three solutions of each compound and the average of these three readings was calculated. Further consistency of molar extinction coefficient (ϵ) was verified using Beer-Lambert law.

Steady State Fluorescence Measurements

The emission spectra of these compounds were recorded on Horiba Fluoromax-4 choosing excitation wavelength $\lambda_{\text{exc}} = 421$ nm in various solvents in dilute (ca. 1.0×10^{-6} M) solutions, at which all of them were soluble. The fluorescence quantum yield values (ϕ) of the compounds were measured using the following relation:

$$\phi_u = \phi_r \frac{F_u A_r \eta_u^2 q_r}{F_r A_u \eta_r^2 q_u}$$

where, 'F' represents the corrected fluorescence peak area, 'A' the absorbance at the excitation wavelength, ' η ' the refractive index of the solvent used, 'q' the excitation light intensity, and the subscripts "r" and "u" refer to reference and unknown respectively. For measuring the relative fluorescence quantum yields of the compounds **2-5** and **8**, coumarin 153 having fluorescence quantum yield of 0.38 in ethanol ($\lambda_{\text{exc}} = 421$ nm), was chosen as the fluorescence quantum yield standard.[7]

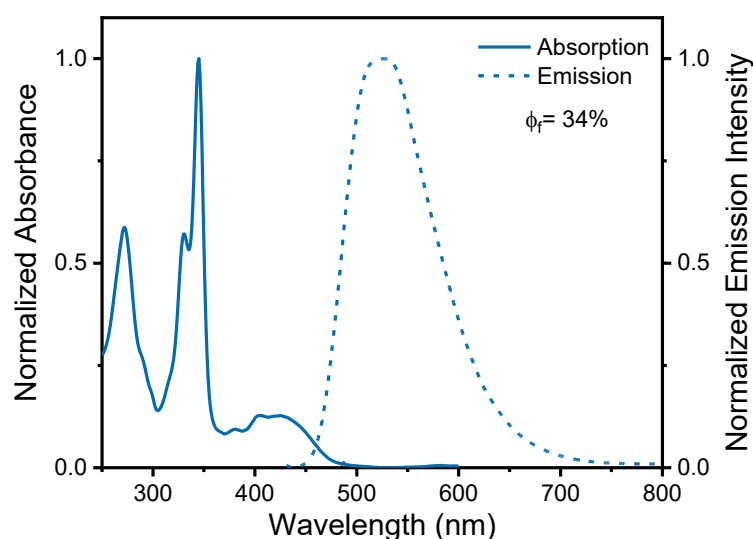


Fig. S14 Absorption (left) and normalized emission (right) spectra of compound **7** in chloroform.

7. Solvatochromism and Dipole Moment Calculations

The carbazole-coumarins **2**, **5** and **8** were examined for their solvatochromic behaviour in different solvents of varying polarity (from low to high polarity).

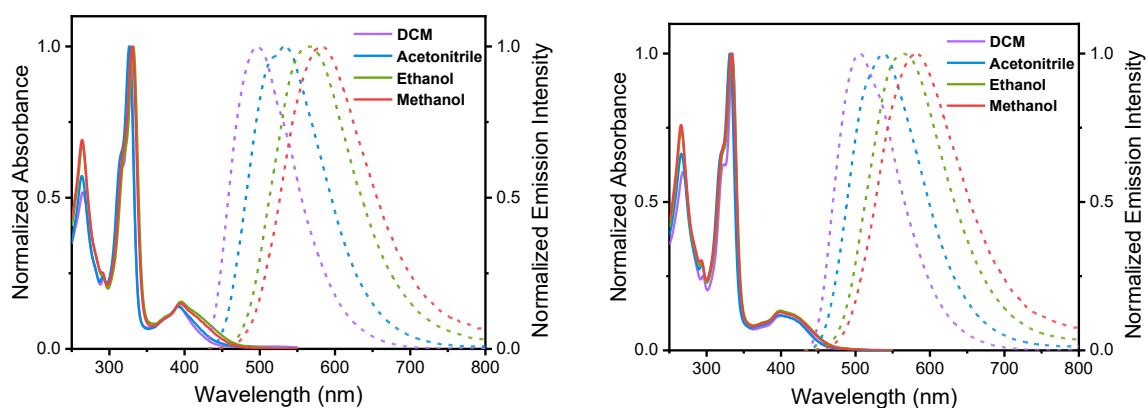


Fig. S15 Normalized absorption and Emission solvatochromic behaviour of compound **2** (left) and **3** (right).

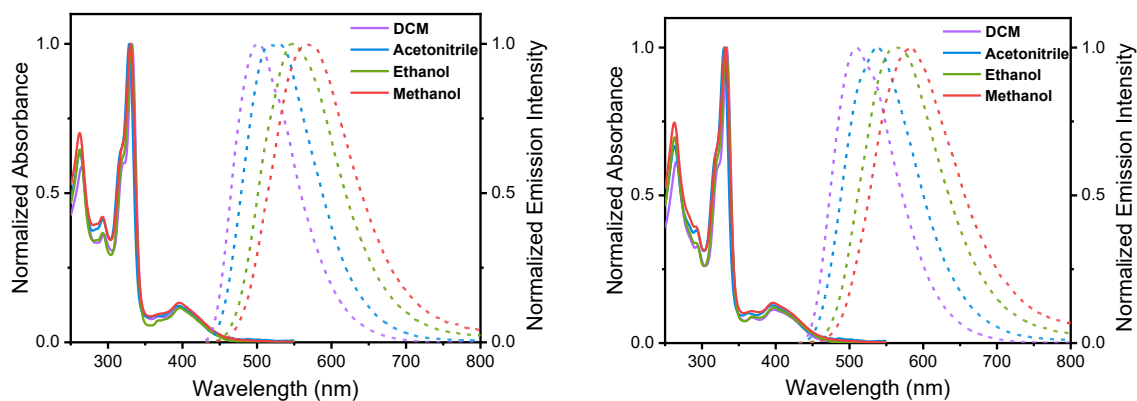


Fig. S16 Normalized absorption and emission solvatochromic behaviour of compound **4** (left) and **5** (right).

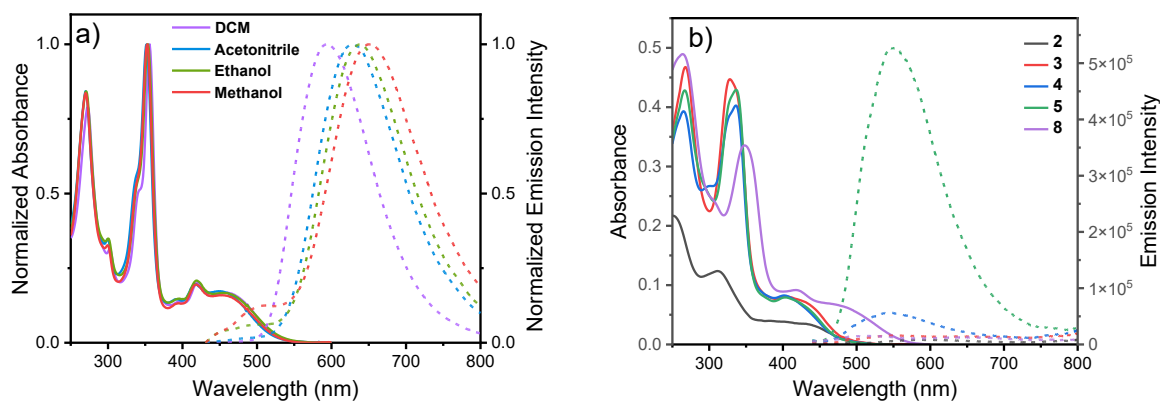


Fig. S17 (a) Normalized absorption and emission solvatochromic behaviour of compound **8**. (b) Absorption and emission spectra of compounds **2-5** and **8** in 5 % DMSO in water medium ($c = 10^{-5}$ M).

Solvatochromism is one of the popular methods known for the determination of the experimental dipole moment of the molecule in the ground and excited states. It can be derived from the absorbance and the emission maximum of the molecule in different solvents, respectively. It is mainly based on the effect of the electric field on the molecule in solution. The ground and excited state dipole moments were calculated following the literature reported method.[8-12]

Table S4. Solvent properties and polarity functions.

Solvent/Polarity function	D ^a	n ^b	f ₁ (D, n) ^c	f ₂ (D, n) ^c	E _T ^N
Chloroform	4.81	1.444	0.371	0.486	0.259
DMSO	46.45	1.476	0.841	0.744	0.444
Toluene	2.38	1.494	0.031	0.349	0.099
DCM	8.93	1.4241	0.590	0.582	0.321
Acetonitrile	37.5	1.3441	0.861	0.665	0.461

Note: ^a Dielectric constant (D) at 25 °C. ^b Refractive index (n) at 25 °C. ^c Polarity functions f₁ (D, n) and f₂ (D, n).

If N_B is the number of bonds, R_A is the number of aromatic rings, and R_{NA} is the number of non-aromatic rings, the Van der Waals volume (V_{vdW}) can be calculated theoretically according to the formula given by Abraham *et al.*, using the atomic and bond contributions of Van der Waals volume.[13]

$$V_{vdW} = \Sigma (\text{all atom contributions}) - 5.92 N_B - 14.7 R_A - 3.8 R_{NA} \quad \dots Eq. 1$$

The number of bonds N_B can be calculated from the formula:

$$N_B = N - 1 + R_A + R_{NA} \quad \dots Eq. 2$$

Where N represents the total number of atoms present in the molecule.

The values of V_{vdW} for atoms carbon, hydrogen, nitrogen and oxygen are calculated to be 20.58, 7.24, 15.60 and 14.71 Å³ respectively. The molecular formula for **2**, **5** and **8** is C₂₀H₁₃NO₂, C₂₇H₁₉NO₃ and C₂₃H₁₆N₂O₂ respectively. The sum of all the atoms Van der Waals volume in the molecule is demonstrated as below.

For **2**,

$$\begin{aligned}\Sigma (\text{all atom contributions}) &= (20 \times 20.58) + (13 \times 7.24) + (15.60 \times 1) + (14.71 \times 2) \\ &= 411.6 + 94.12 + 15.60 + 29.42 \\ &= 550.74\end{aligned}$$

For **5**,

$$\begin{aligned}\Sigma (\text{all atom contributions}) &= (27 \times 20.58) + (19 \times 7.24) + (15.60 \times 1) + (14.71 \times 3) \\ &= 555.66 + 137.56 + 15.60 + 44.13 \\ &= 752.95\end{aligned}$$

For **8**,

$$\begin{aligned}\Sigma (\text{all atom contributions}) &= (23 \times 20.58) + (16 \times 7.24) + (15.60 \times 2) + (14.71 \times 2) \\ &= 473.34 + 115.84 + 31.2 + 29.42 \\ &= 649.8\end{aligned}$$

So, the number of bonds present in the molecule are calculated for **2** and **3** using Eq. 2, and the values comes out to be 124 and 125, respectively. Using the values, the van der Waals volume are calculated.

For **2**,

$$\begin{aligned}V_{vdW} &= \Sigma (\text{all atom contributions}) - 5.92 N_B - 14.7 R_A - 3.8 R_{NA} \\ &= 550.74 - (5.92 \times 40) - (14.7 \times 4) - (3.8 \times 1) \\ &= 550.74 - 236.8 - 58.8 - 3.8 \\ &= 251.34\end{aligned}$$

For **5**,

$$\begin{aligned}V_{vdW} &= \Sigma (\text{all atom contributions}) - 5.92 N_B - 14.7 R_A - 3.8 R_{NA} \\ &= 752.95 - (5.92 \times 55) - (14.7 \times 5) - (3.8 \times 1) \\ &= 752.95 - 325.6 - 73.5 - 3.8 \\ &= 350.05\end{aligned}$$

For **8**,

$$\begin{aligned}
 V_{vdW} &= \Sigma (\text{all atom contributions}) - 5.92 N_B - 14.7 R_A - 3.8 R_{NA} \\
 &= 649.8 - (5.92 \times 47) - (14.7 \times 4) - (3.8 \times 1) \\
 &= 649.8 - 278.24 - 58.8 - 3.8 \\
 &= 308.96
 \end{aligned}$$

Further, assuming a spherical model, if the Onsager radius is 'a', then the van der Waals volume can be represented as:

$$V_{vdW} = \frac{4}{3} \pi a^3 \quad \dots Eq. 3$$

Using this relation, the values for Onsager radius for **2**, **5** and **8** are calculated to be 3.91 Å, 4.37 Å and 4.19 Å, respectively.

Table S5. Molecular data of compounds **2**, **5** and **8**.

Entry	Molecular formulae	Σ (all atom contributions)	N_B	V_{vdw} (Å ³)	a (Å)
2	C ₂₀ H ₁₃ NO ₂	550.74	40	251.34	3.91
5	C ₂₇ H ₁₉ NO ₃	752.95	55	350.05	4.37
8	C ₂₃ H ₁₆ N ₂ O ₂	649.8	47	308.96	4.19

Table S6. Photophysical data of **2** in different solvents.

Solvent	λ_{max} (abs) nm	λ_{max} (em) nm	$\nu_a - \nu_f$ (cm ⁻¹)	$\frac{\nu_a + \nu_f}{2}$ (cm ⁻¹)
Toluene	393	471	4214	23338
Chloroform	393	491	5079	22906
DMSO	396	543	6836	21834
DCM	393	496	5284	22803
Acetonitrile	395	532	6519	22057

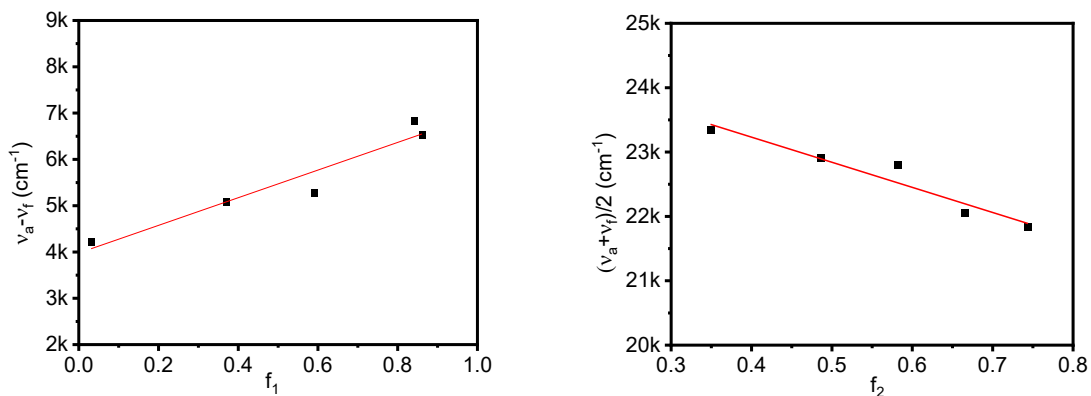


Fig. S18 Plots of polarity functions f_1 and f_2 for different solvents versus solvent shift data of compound **2**.

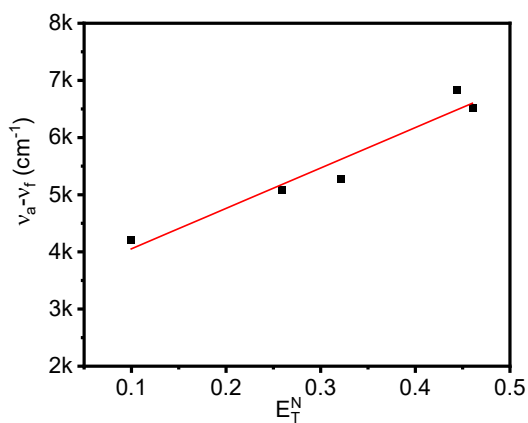


Fig. S19 Plot of solvent parameter E_T^N versus Stokes shift of compound **2**.

Table S7 Photophysical data of **5** in different solvents.

Solvent	λ_{\max} (abs) nm	λ_{\max} (em) nm	$\nu_a - \nu_f$ (cm^{-1})	$\frac{\nu_a + \nu_f}{2}$ (cm^{-1})
Toluene	396	476	4244	23130
Chloroform	398	502	5205	22523
DMSO	396	541	6768	21868
DCM	397	510	5581	22398
Acetonitrile	396	538	6665	21920

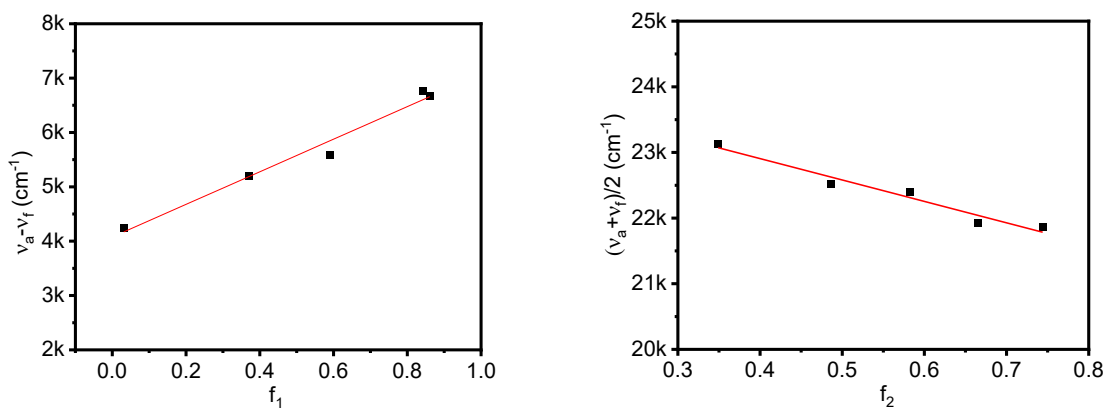


Fig. S20 Plots of polarity functions f_1 and f_2 for different solvents versus solvent shift data of **5**.

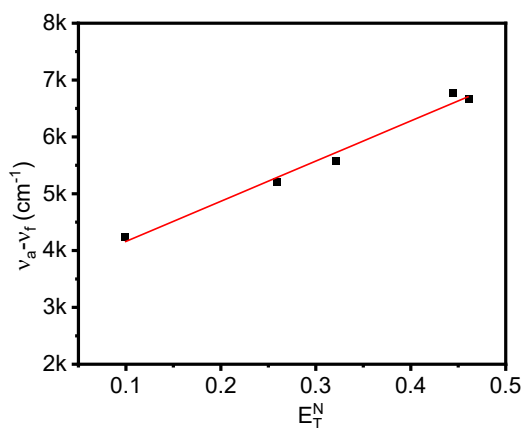


Fig. S21 Plot of Stokes shift versus solvent parameter E_T^N of compound **5**.

Table S8. Photophysical data of **8** in different solvents.

Solvent	λ_{\max} (abs) nm	λ_{\max} (em) nm	$\nu_a - \nu_f$ (cm ⁻¹)	$\frac{\nu_a + \nu_f}{2}$ (cm ⁻¹)
Toluene	447	544	3989	20377
Chloroform	458	587	4798	19435
DMSO	454	560	4169	19942
DCM	460	593	4876	19301
Acetonitrile	451	629	6275	19035

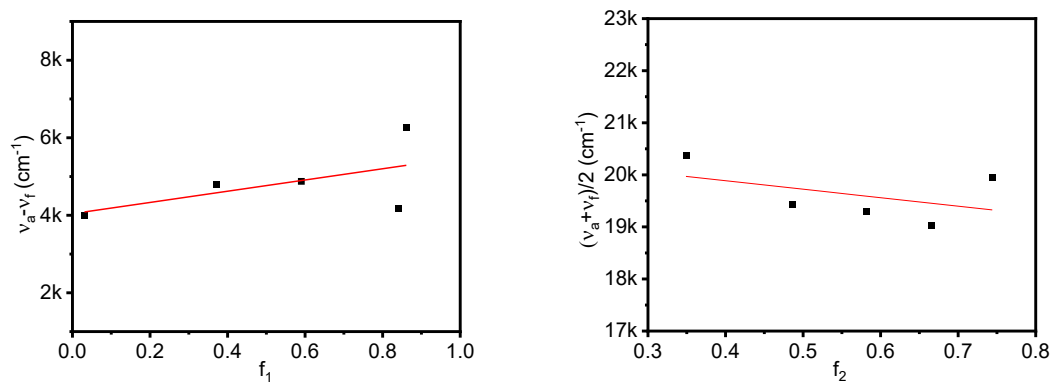


Fig. S22 Plots of polarity functions f_1 and f_2 for different solvents versus solvent shift data of **8**.

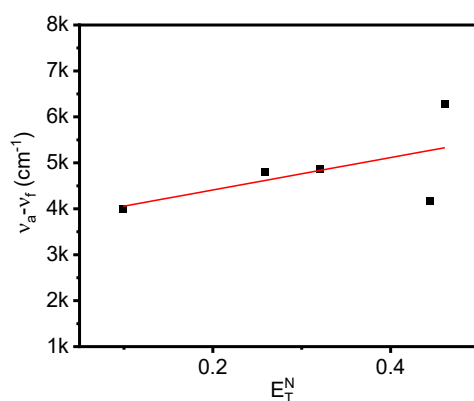


Fig. S23 Plot of Stokes shift versus solvent parameter E_T^N of compound **8**.

Here, initially, the ratio of excited state (μ_e) and ground state (μ_g) dipole moments was determined by utilizing the Bakshiev's equation and Chamma and Viallet equations.[8–9]

Bakshiev formulation,

$$\begin{aligned} \bar{\nu}_a - \bar{\nu}_f &= \frac{2(\mu_e - \mu_g)^2}{a^3 hc} f_1(D, n) + \text{constant} \\ &= S_1 f_1(D, n) + \text{constant} \end{aligned} \quad \dots \text{Eq. 4}$$

Where, S_1 indicates the slope of the linear fit, which was obtained from the $(\bar{\nu}_a - \bar{\nu}_f)$ versus $f_1(D, n)$ and denoted as follows

$$S_1 = \frac{2(\mu_e - \mu_g)^2}{a^3 hc}$$

The Chamma and Viallet equations,

$$\begin{aligned} \frac{(\bar{\nu}_a + \bar{\nu}_f)}{2} &= -\frac{2(\mu_e^2 - \mu_g^2)}{a^3 hc} f_2 (D, n) + constant \\ &= S_2 f_2 (D, n) + constant \end{aligned} \quad \dots Eq. 5$$

Where, S_2 is the slope of the linear fit, which was derived from the $\frac{(\bar{\nu}_a + \bar{\nu}_f)}{2}$ versus $f_2 (D, n)$ and expressed as follows

$$S_2 = -\frac{2(\mu_e^2 - \mu_g^2)}{a^3 hc}$$

In the above equations, $\bar{\nu}_a$ and $\bar{\nu}_f$ are the absorption and fluorescence maxima respectively. n , D , a , h , c indicates refractive indices, dielectric constants of the solvents, Onsager cavity radius, Planck's constant and velocity of light respectively. f indicates the function.

$$f_1 (D, n) = \left[\frac{D-1}{D+2} - \frac{n^2-1}{n^2+2} \right] \left(\frac{2n^2+1}{n^2+2} \right) \quad \dots Eq. 6$$

$$f_1 (D, n) = \frac{1}{2} f_1 (D, n) + \frac{3}{2} \frac{(n^4-1)}{(n^2+2)^2}$$

$$\frac{\mu_e}{\mu_g} = \frac{|S_1 - S_2|}{|S_1 + S_2|}$$

Radhakrishnan and co-workers[10–11]

$$\begin{aligned} \bar{\nu}_a - \bar{\nu}_f &= 11307.6 \left[\left(\frac{\Delta\mu_C}{\Delta\mu_B} \right)^2 \left(\frac{a_B}{a_C} \right)^3 \right] E_T^N + constant \\ &= m E_T^N + constant \end{aligned} \quad \dots Eq. 7$$

Where, m is the slope and obtained from the linear fit of the $(\bar{\nu}_a - \bar{\nu}_f)$ versus E_T^N . It is expressed as follows.

$$m = 11307.6 \left[\left(\frac{\Delta\mu_C}{\Delta\mu_B} \right)^2 \left(\frac{a_B}{a_C} \right)^3 \right]$$

Here, $\Delta\mu_B$ and a_B are the change in the dipole moment and the Onsager cavity radius for the betaine dye, respectively and the values are $\Delta\mu_B = 9 D$ and $a_B = 6.2 \text{ \AA}$. [14] Similarly, $\Delta\mu_C$ and

a_c denotes the dipole moment change and the Onsager cavity radius of the compound **2**, **5** and **8**, respectively.

$$\Delta\mu = (\mu_e - \mu_g) = \sqrt{\frac{m \times 81}{11307.6 \left(\frac{6.2}{a}\right)^3}}$$

From the above, dipole moment ratio $\left(\frac{\mu_e}{\mu_g}\right)$ and difference $(\mu_e - \mu_g)$, the experimental values of ground and excited state dipole moments can be calculated.

Table S9. Experimentally determined ground and excited state dipole moment values of compounds **2**, **5** and **8**.

Property	S1	S2	$\frac{\mu_e}{\mu_g} = \frac{ S_1 - S_2 }{ S_1 + S_2 }$	M	$(\mu_e - \mu_g)$ (D)	μ_e (D)	μ_g (D)
2	2986	-3901	7.53	7068	3.56	4.1	0.54
5	2997	-3262	23.62	7067	4.21	4.40	0.19
8	1448	-1629	17	3526	2.79	2.96	0.17

8. Time-Resolved Fluorescence Measurements

Fluorescence lifetime experiments were performed using Jobin-Yvon TCSPC lifetime instrument having pulsed diode excitation source. The nano-LED of 450 nm was used as the light source for the experiments. The pulse repetition range was fixed to 1.0 MHz and the detector response was around 800 ps. The scatterer (Ludox AS40 colloidal silica) was used to collect the instrument response function and IBH software was used to analyse the decay data. For a good fit, $0.99 \leq \chi^2 \leq 1.3$ was considered along the symmetrical distribution of the residuals. The fluorescence lifetime of the compounds **2–5** and **8** were recorded in chloroform at concentrations, ca. 10^{-6} M.

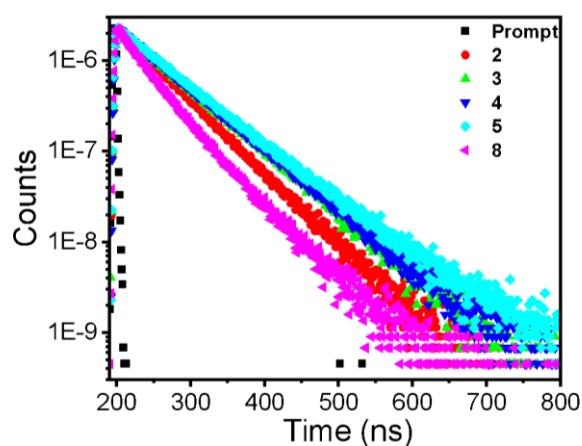


Fig. S24 The fluorescence lifetime decay plot for compounds **2-5**, and **8**.

9. Aggregation Effect

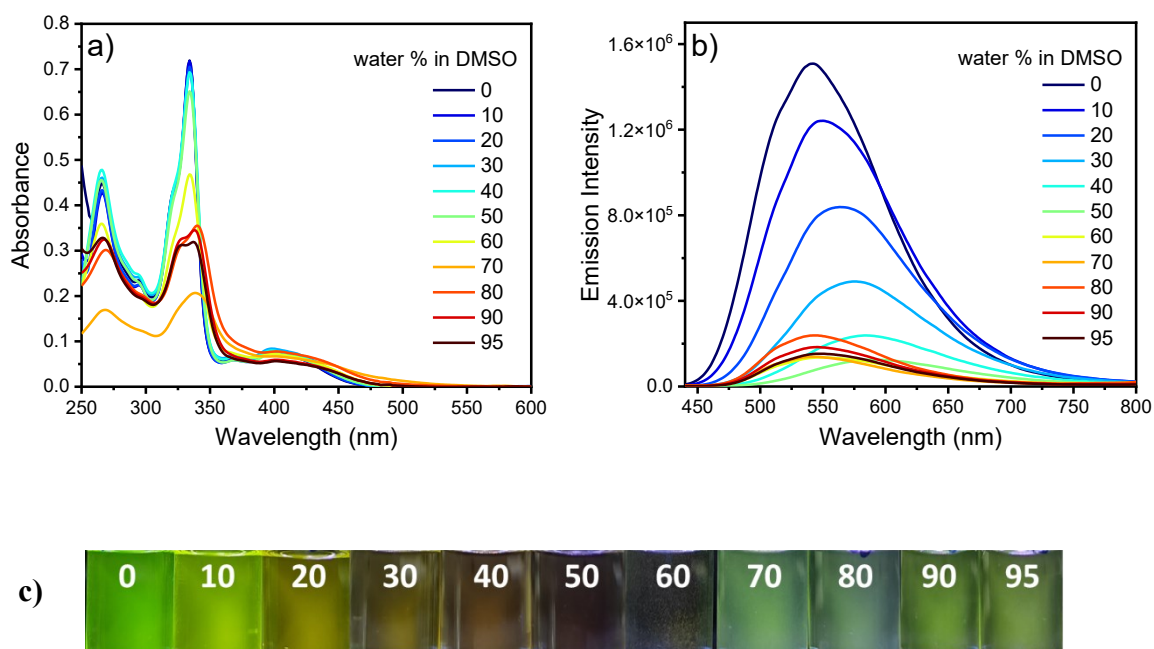


Fig. S25 (a) Absorption spectra of **5** in the DMSO–water mixture and (b) fluorescence spectra in the DMSO–water mixture ($\lambda_{\text{ex}} = 421 \text{ nm}$, $c = 10^{-5} \text{ M}$). (c) Photographs of **5** with varying amounts of water fractions (f_w) under 400 nm excitation in the DMSO–water mixture.

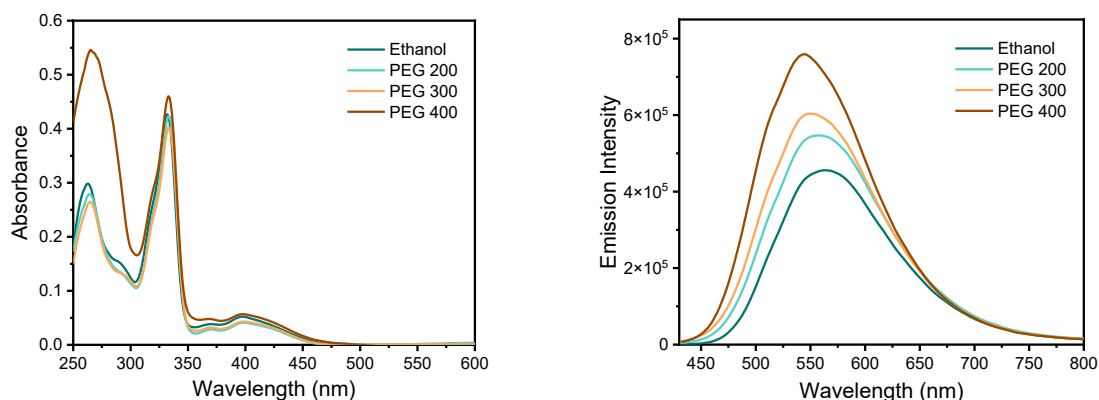


Fig. S26 UV-vis and emission spectral monitoring of **5** in the presence of solvents with increasing viscosity. The viscosities of the solvents increase in the order ethanol < PEG 200 < PEG 300 < PEG 400.

10. Fluorescence Anisotropy Studies. Fluorescence anisotropy value (r) is given by the equation [15]:

$$r = \frac{I_{\parallel} - I_{\perp}}{I_{\parallel} + 2I_{\perp}}$$

Where I_{\parallel} and I_{\perp} are intensities of the emitted light parallel and perpendicular to the direction of the polarized excitation light, respectively. The highest possible value of r is 0.4 for a single photon excitation.

Preparation of Small unilamellar vesicles (SUVs):

SUVs were prepared using the rapid injection method.[16] A stock solution of DMPC and **5** was prepared in ethanol. Then 30 μ L of this ethanol stock solution was injected rapidly into water using a micro-syringe. The resulted solution was equilibrated for 30 minutes at a temperature 45 $^{\circ}$ C; much greater than the phase transition of the liposome. The percentage of ethanol in the solution was less than 1% (v/v). The final concentrations of the lipid and the dye were 0.4 mM and 2 μ M, respectively. The sizes of the prepared DMPC SUVs were measured using Dynamic light scattering (DLS) technique with a SZ-100 Nanopartica, Horiba instrument at 25 $^{\circ}$ C.

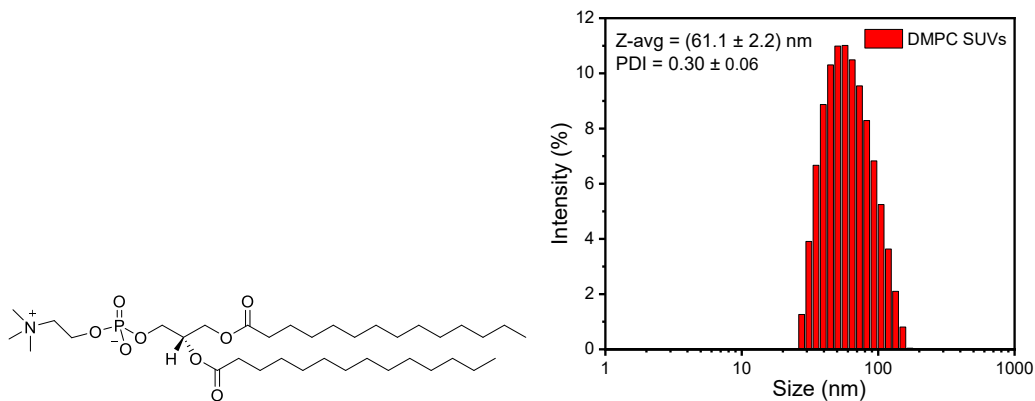


Fig. S27 Structure of 1,2-dimyristoyl-*sn*-glycero-3-phosphocholine (DMPC) lipid (left) and the DLS histogram showing size distributions of the prepared DMPC SUVs (right).

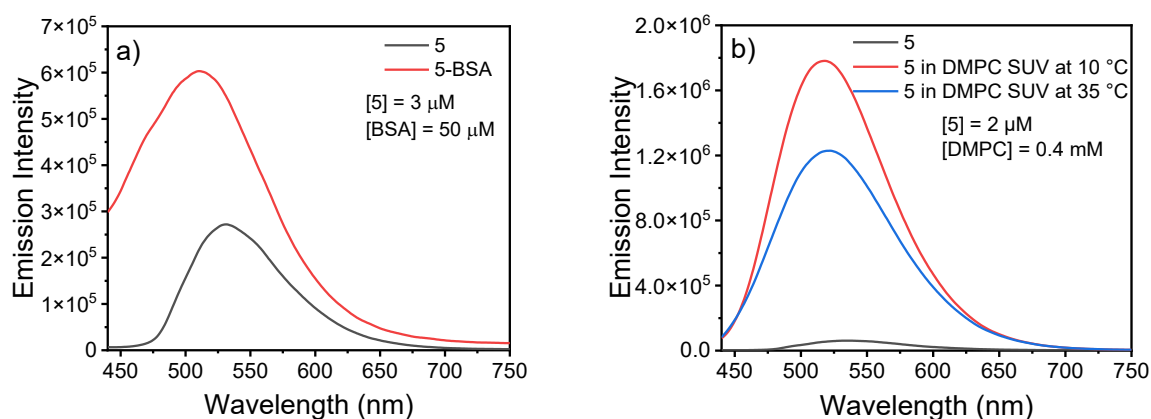


Fig. S28 (a) Steady-state emission spectra of **5** in the absence and presence of bovine serum albumin (BSA) in PBS 7.4. (b) Steady-state emission spectra of **5** in DMPC SUVs at 10 °C (solid gel phase) and 35 °C (liquid crystalline phase) in aqueous medium. $[5] = 2 \mu\text{M}$ and $[\text{DMPC}] = 0.4 \text{ mM}$.

Table S10 Emission wavelengths and fluorescence anisotropies of **5** in only aqueous medium (PBS 7.4), BSA medium, and DMPC SUVs in its solid gel and liquid crystalline phases. (Standard deviations for anisotropy values were within $\pm 3\%$.)

Medium	λ_{em} (nm)	Fluorescence Anisotropy (r)
Aqueous	532	0.02
BSA	510	0.26
DMPC SUV at 10 °C (SG phase)	518	0.17
DMPC SUV at 35 °C (LC phase)	522	0.08

11. Stability and reactivity of Compound 5 under different environment conditions

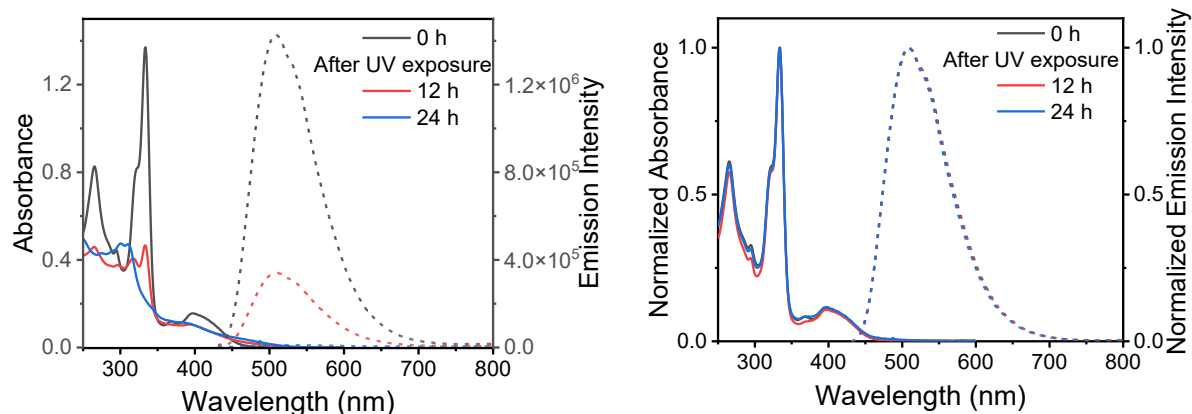


Fig. S29 UV-vis and emission spectral monitoring of **5** in aerated CHCl_3 solution before and after exposure to UV radiation for 24 h in solution state (left) and in solid state (right).

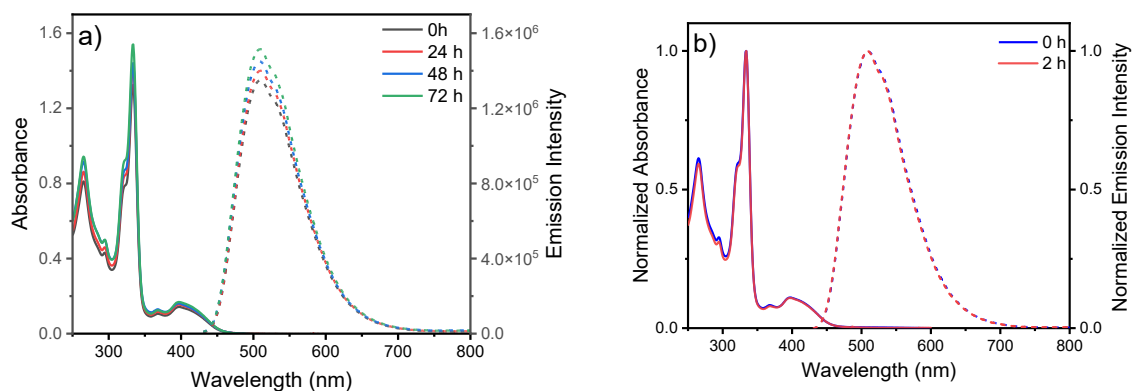


Fig. S30 UV-vis and emission spectral monitoring of **5** in aerated CHCl_3 solution before and after exposure to a) room light under air, b) heating at 100°C for 2 hours under N_2 atmosphere.

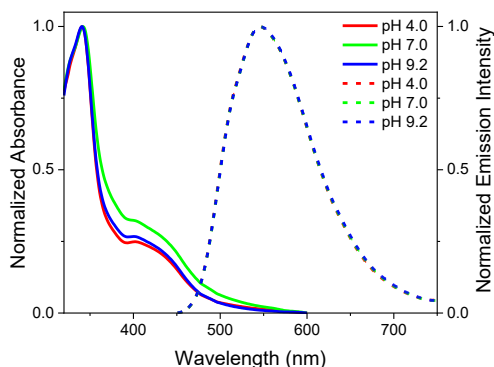


Fig. S31 UV-vis and emission spectral monitoring of **5** in aerated 5% DMSO in water medium at acidic (4.0), neutral (7.0) and basic pH (9.2).

12. Electrochemical Studies

Electrochemical properties of carbazole-coumarins **2-5**, and **8** were measured at a scan rate of 0.1 V/s using 0.1 M of tetra-*n*-butylammonium hexafluorophosphate (TBAPF₆) as supporting electrolyte dissolved in nitrogen-purged dry dichloromethane with a CH Instruments 660A potentiostat using glassy carbon as working electrode and an Ag/Ag⁺ (0.01 M) as reference electrode at room temperature. The measurements were calibrated using ferrocene as an external standard. The formula used for HOMO-LUMO calculation from CV are $E_{\text{HOMO}} = [E_{\text{ox}} - E_{1/2}(\text{Fc}) + 4.8]$ eV, $E_{\text{LUMO}} = [E_{\text{red}} - E_{1/2}(\text{Fc}) + 4.8]$ eV and $E_g = [E_{\text{LUMO}} - E_{\text{HOMO}}]$ eV, and the $E_{\text{LUMO}}(\text{opt})$ was calculated from $E_g = 1240/\lambda_{\text{onset}}$.

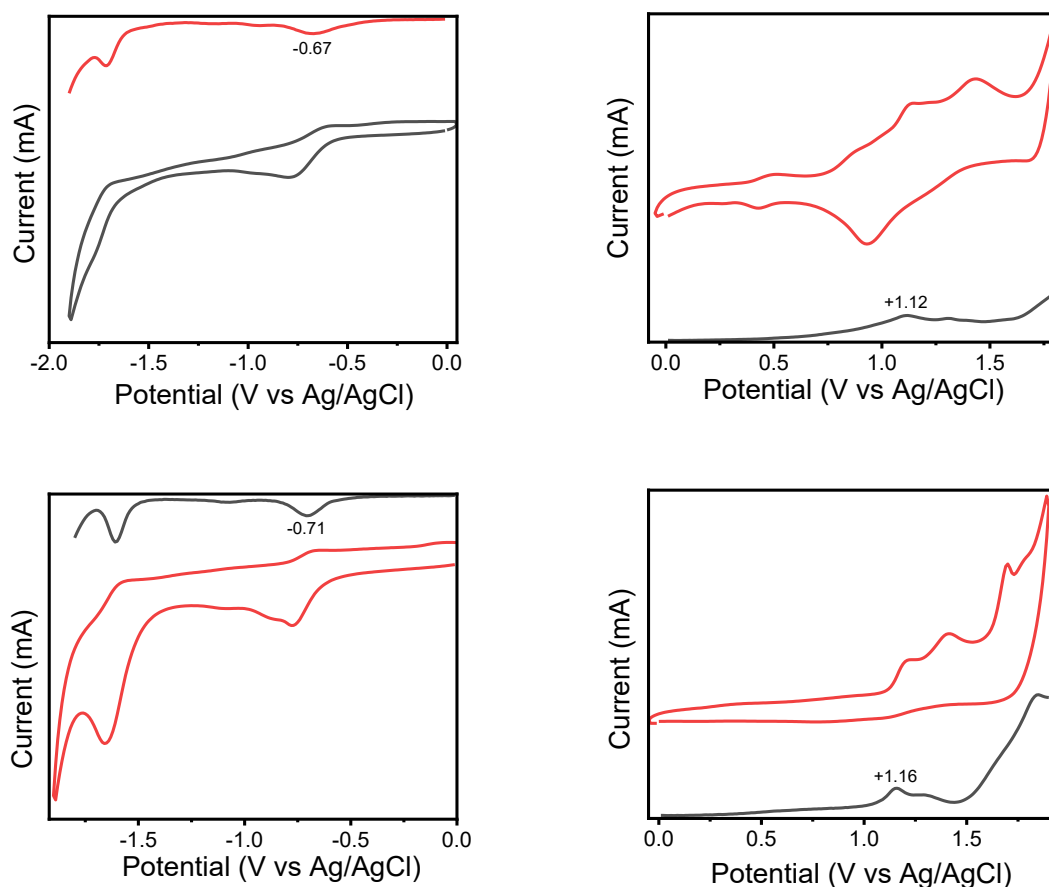


Fig. S32 Cyclic voltammograms of **2** (first row), **3** (second row), in dichloromethane.

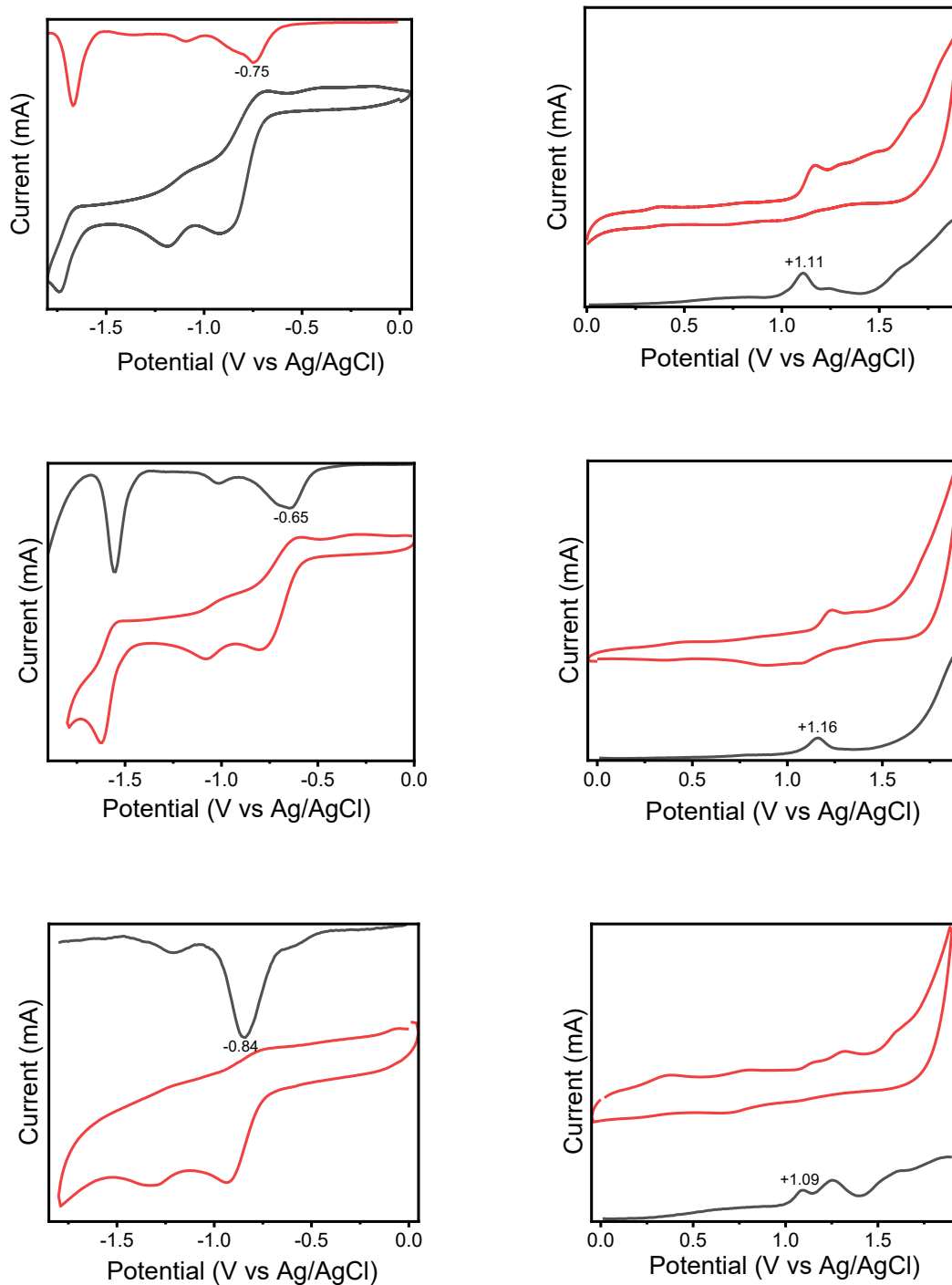


Fig. S33 Cyclic voltammograms of **4** (first row), **5** (second row) and **8** (third row) in dichloromethane.

Table S11 Electrochemical data from cyclic voltammetry recorded in dry DCM using TBAPF₆ as the supporting electrolyte. The oxidation and reduction potentials (in V) were measured against the reference electrode Ag/AgCl. Calculated using $E_{\text{HOMO}} = [E_{\text{ox}} - E_{1/2}(\text{Fc}) + 4.8]$ eV, $E_{\text{LUMO}}(\text{CV}) = [E_{\text{red}} - E_{1/2}(\text{Fc}) + 4.8]$ eV and $E_{\text{g}}(\text{CV}) = [E_{\text{LUMO}}(\text{CV}) - E_{\text{HOMO}}]$ eV, $E_{\text{g}}(\text{Opt}) = (1240/\lambda_{\text{onset}})$ eV (using DCM as solvent) and $E_{\text{LUMO}}(\text{Opt}) = [E_{\text{g}}(\text{Opt}) + E_{\text{HOMO}}]$ eV.

Compound	E_{ox} (V)	E_{red} (V)	E_{HOMO} (eV)	$E_{\text{LUMO}}(\text{opt})$ / $E_{\text{LUMO}}(\text{CV})$ (eV)	$E_{\text{g}}(\text{opt})$ / $E_{\text{g}}(\text{CV})$ (eV)
2	+1.12	-0.67	-5.36	-2.48/-3.66	2.88/1.70
3	+1.16	-0.71	-5.40	-2.70/-3.62	2.70/1.78
4	+1.11	-0.75	-5.35	-2.63/-3.58	2.72/1.77
5	+1.16	-0.65	-5.40	-2.70/-3.68	2.70/1.72
8	+1.11	-0.84	-5.51	-3.16/-3.56	2.35/1.95

13. DFT Calculated FMOs and Energies

The optimization of molecules is carried out by utilizing theoretical methods and employing Density Functional Theory (DFT) calculations. The software involved in optimizing the electronic ground state geometry of molecules in gas phase without any symmetric considerations are Gaussian 16 and B3LYP functional in 6-31G(d) basis set.[16–18]

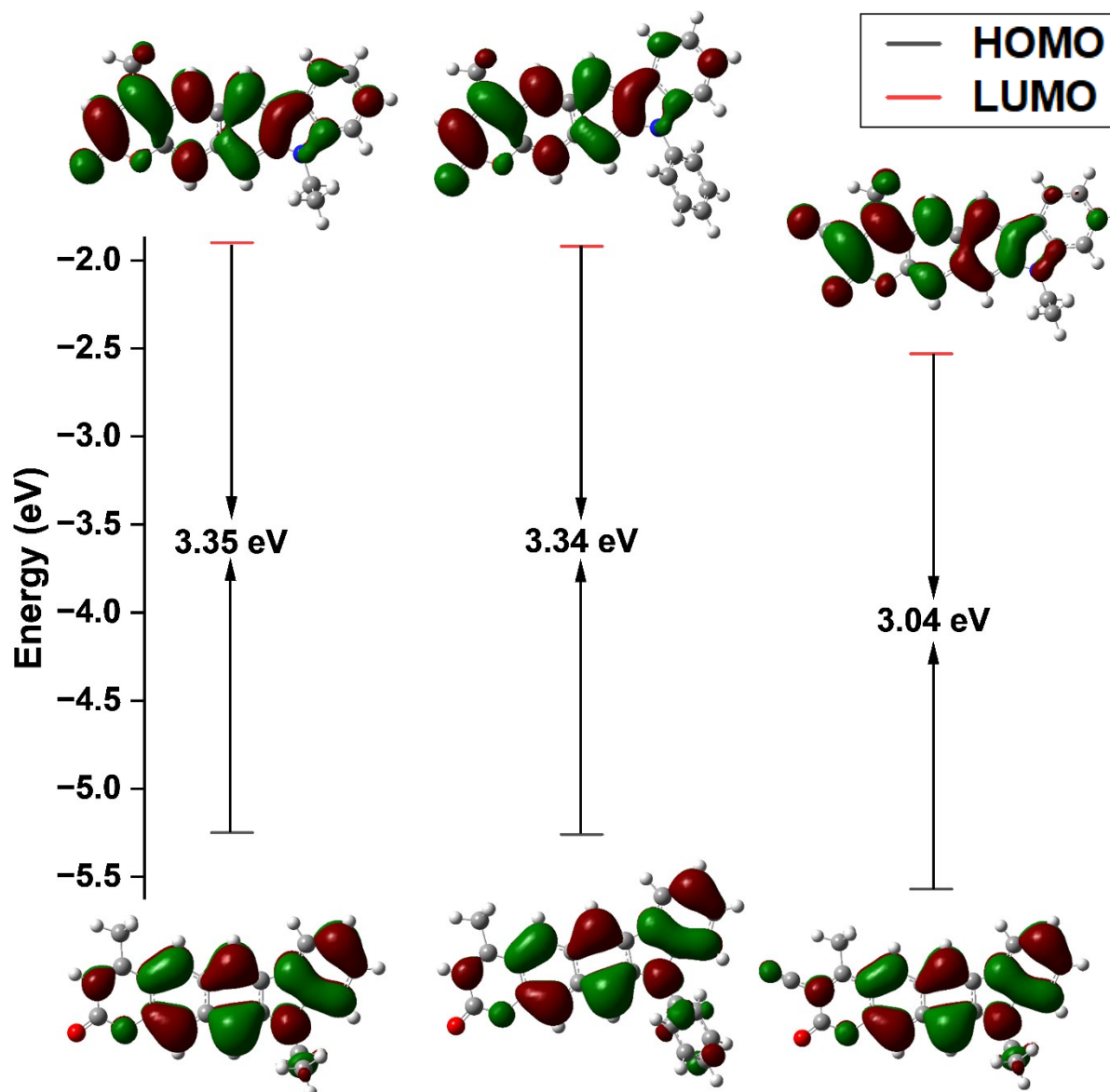


Fig. S34 Calculated frontier molecular orbitals (FMOs) of carbazole-fused coumarins **3**, **4** and **8** (left to right), respectively in gas phase.

14. References

1. Q. Zhang, P. Jiang, K. Wang, G. Song and H. Zhu, *Dyes and Pigments*, 2011, **91**, 89–97.
2. W. Jiang, L. Duan, J. Qiao, G. Dong, D. Zhang, L. Wang and Y. Qiu, *J. Mater. Chem.*, 2011, **21**, 4918–4926.
3. K. M. Kim and I. H. Park, *Synthesis* (Stuttg), 2004, 2004, 2641–2644.
4. S. Lele, M. G. Patel and S. Sethna, *J. Org. Chem.*, 1962, **27**, 637–639.

5. G. M. Sheldrick, SADABS. Program for Empirical Absorption Correction. University of Gottingen, Germany. 1996
6. G. M. Sheldrick, SHELXTL Version 2014/7. <http://shelx.uniuc.gwdg.de/SHELX/index.php>. 2014.
7. G. Jones, W. R. Jackson, C. Y. Choi and W. R. Bergmark, *J. Phys. Chem.*, 1985, **89**, 294–300.
8. N. G. Bakhshiev, *Opt. Spektosk. (USSR)*, 1964, **16**, 821.
9. A. Chamma and P. Viallet, *CR. Hebd. Seanc. Acad. Sci. Ser.*, 1970, **270**, 1901.
10. K. Chandrasekhar, L. R. Naik, H. M. Suresh Kumar and N. N. Math, *Ind. J. Pure Appl. Phys.*, 2006, **44**, 292.
11. M. Ravi, A. Samanta and T. P. Radhakrishan, *J. Phys. Chem.*, 1994, **98**, 9133.
12. M. Ravi, T. Soujanya, A. Samanta and T. P. Radhakrishan, *J. Chem. Soc. Faraday Trans.*, 1995, **91**, 2739.
13. Y. H. Zhao, M. H. Abraham and A. M. Zissimos, *J. Org. Chem.*, 2003, **68**, 7368.
14. C. Reichardt, *Solvents and Solvent Effect in Organic Chemistry*, VCH, Weinheim, 1988.
15. J. R. Lakowicz, *Principles of fluorescence spectroscopy*, Springer, 2006.
16. T. Shyamala and A. K. Mishra, *Photochem. Photobiol.*, 2004, **80**, 309–315.
17. M. J. Frisch, G. W. Trucks, H. B. Schlegel, G. E. Scuseria, M. A. Robb, J. R. Cheeseman, G. Scalmani, V. Barone, B. Mennucci, G. A. Petersson, H. Nakatsuji, M. Caricato, X. Li, H. P. Hratchian, A. F. Izmaylov, J. Bloino, G. Zheng, J. L. Sonnenberg, M. Hada, M. Ehara, K. Toyota, R. Fukuda, J. Hasegawa, M. Ishida, T. Nakajima, Y. Honda, O. Kitao, H. Nakai, T. Vreven, Jr J. A. Montgomery, J. E. Peralta, F. Ogliaro, M. Bearpark, J. J. Heyd, E. Brothers, K. N. Kudin, V. N. Staroverov, R. Kobayashi, J. Normand, K. Raghavachari, A. Rendell, J. C. Burant, S. S. Iyengar, J. Tomasi, M.

Cossi, N Rega, J. M. Millam, M. Klene, J. E. Knox, J. B. Cross, V. Bakken, C. Adamo, J. Jaramillo, R. Gomperts; R. E. Stratmann, O. Yazyev, A. J. Austin, R. Cammi, C. Pomelli, J. W. Ochterski, R. L. Martin, K. Morokuma, V. G. Zakrzewski, G. A. Voth, P. Salvador, J. J. Dannenberg, S. Dapprich, A. D. Daniels, O. Farkas, J. B. Foresman, J. V. Ortiz, J. Cioslowski, D. J. Fox, Gaussian 16, Revision B.01; Gaussian, Inc.: Wallingford, CT, 2016.

18. A. D. Becke. *J. Chem. Phys.* 1993, **98**, 5648-5652.
19. C. Lee, W. Yang and R. G. Parr *Phys. Rev. B.* 1988, **37**, 785-789.
